UNIVERSIDADE FEDERAL DO RIO GRANDE DO SUL
ESCOLA DE ENGENHARIA
PROGRAMA DE PÓS-GRADUAÇÃO EM ENGENHARIA DE MINAS METALÚRGICA E DE MATERIAIS - PPGE3M
LABORATÓRIO DE TECNOLOGIA MINERAL E AMBIENTAL - LTM

ESTUDOS DE GERAÇÃO E CARACTERIZAÇÃO FÍSICO-QUÍMICA DE NANOBOLHAS PRODUZIDAS POR DESPRESSURIZAÇÃO E APLICAÇÕES EM SISTEMAS DE FLOTAÇÃO

TESE DE DOUTORADO

M.Sc. André Camargo de Azevedo

Porto Alegre
2017

UNIVERSIDADE FEDERAL DO RIO GRANDE DO SUL
ESCOLA DE ENGENHARIA
PROGRAMA DE PÓS-GRADUAÇÃO EM ENGENHARIA DE MINAS METALÚRGICA E DE MATERIAIS - PPGE3M
LABORATÓRIO DE TECNOLOGIA MINERAL E AMBIENTAL - LTM

ESTUDOS DE GERAÇÃO E CARACTERIZAÇÃO FÍSICO-QUÍMICA DE NANOBOLHAS PRODUZIDAS POR DESPRESSURIZAÇÃO E APLICAÇÕES EM SISTEMAS DE FLOTAÇÃO

1
André Camargo de Azevedo

Tese apresentada ao programa de pós-graduação em engenharia de Minas, Metalúrgica e de Materiais da Universidade Federal do Rio Grande do Sul, como requisito parcial à obtenção do título de doutor em engenharia.
Área de concentração: Tecnologia Mineral, Ambiental e Metalurgia Extrativa
Orientador:
Prof. Dr. Jorge Rubio

Porto Alegre
2017

“Não sei de nenhum momento da história da humanidade em que a ignorância foi melhor que o conhecimento”

Neil deGrase Tyson

Esta Tese será julgada para a obtenção do título de Doutor em Engenharia, área de concentração em Tecnologia Mineral, Ambiental e Metalurgia Extrativa pela seguinte Banca Examinadora do Curso de Pós-Graduação.

ORIENTADOR: PROF. DR. JORGE RUBIO

BANCA EXAMINADORA:

PROF. DR. ANDREA MOURA BERNARDES (PPGE3M – UFRGS)
DR. RAFAEL NEWTON ZANETI (DMAE)
PROF. DR. RENATO DANTAS ROCHA DA SILVA (IFRN)

Prof. Dr. Carlos Pérez Bergmann
Coordenador do PPGE3M/UFRGS

AGRADECIMENTOS

Às instituições MCTI/CNPq e MEC/UFRGS/PPGE3M, pela bolsa de auxílio, pela verba para pesquisa, pelo suporte nas publicações e congressos e pela estrutura de excelência.

Aos meus pais, Victor e Maria Inêz, pelo apoio incondicional ao longo de toda minha formação.

Aos meus irmãos, Laís, José Victor, Túlio e Érico, pela amizade e companheirismo nas horas difíceis.

À minha afilhada, Lívia, por ter vindo ao mundo e enchido nossa família de luz e alegria.

Ao Laboratório de Tecnologia Mineral e Ambiental - LTM, na pessoa do seu coordenador – Jorge Rubio, pelo *Know-how* e *know-why* que me foram transmitidos.

Às empresas Vale S.A. e Hidrocicle, pela parceria na execução de projetos que possibilitaram a aquisição de equipamentos e infraestrutura do LTM que possibilitaram a realização desse trabalho.

Aos professores e colaboradores, Ivo Schneider, Adriana Pohlmann, Alexandre Englert, pelo apoio técnico e realização de análises para execução do trabalho.

Em especial aos colegas e amigos do LTM, Ramiro Etchepare, Henrique Oliveira, Cassiano Rossi, Márcio Nicknig, Selma Calgaroto, Juarez Amaral, Beatriz Firpo, Meise Paiva, Ana Flávia Rosa, Jaqueline Mohr e todos os outros que direta ou indiretamente colaboraram na realização do trabalho.

A todos os alunos bolsistas de Iniciação Científica do LTM, especialmente para Luísa Neves, Luciana Kaori, Claudio Backes e Gabriele Leão, que foram peças fundamentais na execução da metodologia experimental.

Aos amigos e colaboradores, Marcelo Fermann, Rafael Zaneti e Alex Rodrigues, por todo apoio técnico na montagem dos sistemas experimentais e discussões técnicas.

RESUMO

O presente trabalho descreve um estudo teórico-experimental da geração de nanobolhas (NBs) por despressurização, da caracterização físico-química das dispersões aquosas de NBs e seus efeitos nos sistemas de flotação de minérios e efluentes líquidos, nas etapas de agregação, condicionamento e flotação. A geração de NBs foi realizada em um sistema de bancada de Flotação por Ar Dissolvido (FAD), por despressurização de uma corrente aquosa supersaturada em ar em um constritor de fluxo (válvula agulha), onde ocorre o fenômeno de cavitação hidrodinâmica com geração de microbolhas (MBs) e NBs. Após, um procedimento de separação das NBs em uma coluna de vidro foi realizado, explorando o fato de que as MBs ascendem e colapsam na superfície do líquido, enquanto as NBs são estáveis e permanecem em suspensão por longos períodos de tempo. As dispersões aquosas de NBs foram caracterizadas medindo diversos parâmetros físicos e físico-químicos, entre outros: concentração numérica, diâmetro médio-Dm, potencial zeta-PZ e tempo de vida. Para tanto, foram usadas as técnicas de Nanoparticle Tracking Analysis (NTA, ZetaView®, Particle Matrix, Germany) e Dynamic Light Scattering (DLS, NanoZetaSizer®, Malvern, UK). Ainda, foram avaliadas diferentes condições de geração para os parâmetros pressão de saturação e tensão superficial da solução aquosa. Os resultados demonstraram que a concentração de NBs é inversamente proporcional a pressão de saturação e a tensão superficial do líquido, atingindo o valor de $1{,}6 \times 10^{9}$ NBs.mL^{-1} com Psat = 2,5 bar e solução de alfa-Terpineol (100 mg.L^{-1} e Tsup = 49 mN.m^{-1}). Ainda, medidas de NTA demonstraram que as NBs permanecem estáveis, sem mudanças significativas na sua concentração numérica e no tamanho médio, por um período superior a 14 dias. Ainda, com o preparo de amostra da dispersão aquosa de NBs com uso de corante azul de metileno, foi possível a realização de microfotografias de dispersões aquosas de NBs, uma vez que o corante adsorve na superfície das bolhas e possibilita um contraste visual necessário para obtenção de imagens por microscopia ótica. As interações de NBs com partículas minerais, precipitados coloidais de aminas e microbolhas foram estudadas, assim como seus efeitos na flotação aplicada a esses sistemas (partículas de quartzo e precipitados de aminas). Os resultados de flotação mostraram que as nanobolhas isoladas não são capazes de flotar as partículas de quartzo, devido ao baixo *lifting power* das NBs. Entretanto, quando utilizadas em uma etapa de condicionamento do quartzo, antes da flotação com macrobolhas, foram responsáveis por aumentar significativamente a flotação de partículas finas (<37 μm) em cerca de 20%. Porém, esse mesmo efeito não foi observado na recuperação das partículas grossas (> 212 μm). Os precipitados de amina foram formados em meio alcalino (insolubilização) a partir

de concentração 10^{-3} mol.L^{-1}, pH >10,5 e após 30 min de agitação. As medidas de tamanho e potencial zeta, em função do pH do meio, mostraram que os colóides formados apresentaram tamanhos na ordem de nanômetros (120 – 350 nm), sendo que o máximo crescimento foi obtido próximo ao ponto isoelétrico (pH 11). Os estudos de flotação dos precipitados coloidais de amina revelaram que as nanobolhas isoladas foram altamente eficientes, atingindo valores de remoção em torno de 80%. Por sua vez, a flotação com microbolhas juntamente com as nanobolhas apresentaram valores de remoção de amina entre 50 – 60 %. Para validar os resultados obtidos previamente dos efeitos das NBs na flotação de quartzo e precipitados coloidais de aminas, foram realizados estudos com condicionamento de partículas finas de quartzo (D_{32} = 8 μm) e de precipitados de aminas com NBs e análise por microscopia ótica (magnificação de 1000x), demonstrando visualmente a agregação desses sistemas particulados. Acredita-se que a presente Tese de doutorado traz avanços na geração de NBs dispersas em alta concentração e apresenta dados inéditos de caracterização física e físico-química desses sistemas, contribuindo para um melhor entendimento dos efeitos das NBs em diferentes sistemas de flotação no tratamento de minérios e de efluentes líquidos e possibilitando o desenvolvimento de novas técnicas que utilizam NBs em diferentes áreas da engenharia e outras ciências aplicadas.

ABSTRACT

The present work describes a theoretical and experimental study of the generation of nanobubbles (NBs) by depressurization, the physico-chemical characterization of aqueous dispersions of NBs and its effects on flotation systems of minerals and liquid effluents, in the steps of aggregation, conditioning and flotation. The generation of NBs was performed in a bench system of Dissolved Air Flotation (DAF) for depressurizing an aqueous stream supersaturated in air at a flow constrictor (needle valve), where the hydrodynamic cavitation phenomenon generating microbubbles (MBs) and NBs occurs. After, a separation procedure of NBs in a glass column was accomplished by exploiting the fact that the MBs rise and collapse on the liquid surface, while the NBs are stable and remain suspended in the liquid for long periods of time. The aqueous dispersions of NBs were characterized by measuring physical and physicochemical parameters, among others: numerical concentration, mean diameter-Dm, zeta potential-PZ and lifetime. For that, it was used the techniques of Nanoparticle Tracking Analysis (NTA, ZetaView®, Particle Matrix, Germany) and Dynamic Light Scattering (DLS, NanoZetaSizer®, Malvern, UK). Different conditions for the generation of NBs were evaluated for the parameters of saturation pressure and surface tension of the aqueous solution. The results showed that the concentration of NBs is inversely proportional to the saturation pressure and the surface tension of the liquid, reaching the value of 1.6×10^9 NBs mL^{-1} with Psat = 2.5 bar and alpha-terpineol solution (100 mg L^{-1} and surface tension = 49 mN m^{-1}). Yet, measurements by NTA technique showed that NBs are stable without significant changes in their number concentration and their mean size, for a period of at least 14 days. Furthermore, with the use of methylene blue dye in the preparation of the sample of aqueous dispersion of NBs, it was possible to perform photomicrographs of aqueous dispersions of NBs, since the colorant adsorbs on the surface of the bubbles and provides a visual contrast needed to obtain pictures by optical microscopy. The NBs interactions with mineral particles (quartz), colloidal amines precipitates and microbubbles were studied, as well as its effects on flotation applied to these systems (quartz particles and amines precipitates). The results showed that flotation with isolated nanobubbles are not able to float quartz particles due to the low lifting power of NBs. However, when used in a conditioning step of the quartz particles prior to the flotation with macrobubbles, the NBs were responsible for significantly increasing the flotation of fine quartz particles (< 37 mm) by about 20%. However, the same effect was not observed in the recovery of coarse particles (> 212 μm) The amines precipitates were formed in alkaline medium (insolubilization) with a concentration of 10^{-3} mol L^{-1} and pH > 10.5, after 30 min of stirring.

The size and zeta potential measurements as a function of pH, showed that the colloids formed had sizes in the nanometer range (120-350 nm), and maximum growth was obtained near the isoelectric point (pH 11). Flotation studies of amines colloidal precipitates revealed that the isolated nanobubbles were highly efficient, reaching values of amine removal near 80%. On the other hand, the flotation with microbubbles jointly with nanobubbles presented amines removal efficiency about 50 – 60 %. To validate previously obtained results of the effects of NBs in the flotation of quartz and amines colloidal precipitates, studies were performed with conditioning of fine quartz particles (D32 = 8 microns) and precipitated amines with NBs and analysis by optical-microscopy (magnification 1000x), visually demonstrating the aggregation of these particulate systems. It is believed that this doctoral thesis provides advances in the generation of dispersed NBs at high concentration and provides novel data of physical and physicochemical characterization of such systems and contributes to a better understanding of the effects of NBs in different flotation systems in the beneficiation of minerals and the treatment of liquid effluents and enabling the development of new techniques that use NBs in different areas of engineering and other applied sciences.

SUMÁRIO

LISTA DE FIGURAS

LISTA DE TABELAS

LISTA DE SÍMBOLOS

ΔF – Energia requerida na formação de bolhas de ar

γ - Tensão Superficial

AFM – *Atomic Force Microscopy*

D32 – Diâmetro Médio de Sauter (volumétrico)

D50 – Diâmetro médio aritmético

DAF – *Dissolved Air Flotation*

DI - Deionizada

DLS – *Dynamic Light Scattering*

FAD – Flotação por Ar Dissolvido

FAI – Flotação por Ar Induzido

F-NBs – Flotação com nanobolhas isoladas

INPI - Instituto Nacional da Propriedade Industrial

LTM – Laboratório de Tecnologia Mineral e Ambiental

MBs – Microbolhas

NBs – Nanobolhas

NTA – *Nanoparticle Tracking Analysis*

P_o – Pressão Atmosférica

P+L – Produção mais limpa

P&D&I – Pesquisa, desenvolvimento e inovação

PAC – Policloreto de Alumínio

Psat – Pressão de Saturação

PZ – Potencial Zeta

Rpm – Rotações por minuto

TIRFM – *Total Internal Reflection Fluorescence Microscopy*

Tsup – Tensão Superficial

UFRGS – Universidade Federal do Rio Grande do Sul

PARTE I

1. INTRODUÇÃO

Nanobolhas (NBs) ocorrem como unidades de gás altamente estáveis adsorvidas em superfícies sólidas (NBs interfaciais ou superficiais) e espalham-se como estruturas semelhantes a panquecas ou dispersões líquidas (*bulk NBs*). O primeiro relato de NBs interfaciais é um trabalho experimental que mediu a força atrativa entre superfícies hidrofóbicas imersas em água (Parker et al., 1994). Consequentemente, este comportamento é uma função escalonada da distância de separação entre as superfícies, que é atribuída à presença de bolhas submicrométricas que ligam as superfícies. Posteriormente, uma evidência experimental da existência de NBs foi fornecida por Miller et al. (1999), que usaram a espectroscopia de infravermelho de transformada de Fourier (FTIR) para investigar a água saturada com n-butano em contato com a superfície sólida de um silicone hidrofóbico. Estas medidas revelaram a acomodação de gás butano na interface sólido/líquido.

Os métodos de geração, estudos básicos e aplicações das nanobolhas (NBs) constituem áreas de pesquisa emergentes e em acelerado crescimento, especialmente nas últimas duas décadas. O elevado potencial tecnológico das NBs em diversas áreas de conhecimento (medicina, agronomia, engenharias) é atribuído principalmente a importantes peculiaridades nas suas propriedades físicas, químicas, físico-químicas e biológicas, das quais podemos destacar a alta estabilidade, longevidade e rápida adesão em superfícies hidrofóbicas.

Embora o potencial tecnológico da utilização de NBs de gases em líquidos em diversas áreas seja enorme, ainda são muito poucas as aplicações dessas tecnologias em escala real, principalmente nas áreas de engenharia, estando ainda limitadas ao setor acadêmico, em fase de pesquisa e desenvolvimento de tecnologias para transferência aos setores produtivo e de serviços. A Tabela 1.1 mostra os principais trabalhos desenvolvidos para aplicação de NBs em diversas áreas do conhecimento.

Tabela 1.1. Áreas de estudos com trabalhos publicados de aplicação de nanobolhas.

Área de estudo	Observações	Referências
Agronomia e criação de animais aquáticos	Caracterização das propriedades físico-químicas e bioativadoras da água contendo NBs. Efeitos das NBs na germinação de sementes e crescimento de plantas de cevada	(Liu et al., 2013; S. Liu et al., 2012; Oshita and Liu, 2013)
	Efeitos de NBs no transporte de água em tecidos vegetais	(Schenk et al., 2015)

	Sistemas de cultivo hidropônico de plantas e criação de animais aquáticos com água rica em NBs	(Ebina et al., 2013; Takahashi and Chiba, 2007)
Remediação de ambientes aquáticos degradados	Efeitos de NBs na recuperação de ambientes de águas superficiais e subterrâneas	(Li et al., 2014, 2013; Nakashima et al., 2012)
Limpeza e desincrustação de superficies sólidas	Limpeza de superfícies metálicas e poliméricas	(Chen et al., 2009; Liu et al., 2008; Liu and Craig, 2009; Wu et al., 2008; Yang and Duisterwinkel, 2011a; Zhu et al., 2016)
	Limpeza de tecidos	(Ushida et al., 2012b)
	Defouling de membranas cerâmicas e poliméricas	(Ghadimkhani et al., 2016)
Medicina e odontologia	NBs como agentes de contraste em utrasonografia	(Mai et al., 2013; Reshani H. Perera et al., 2014; Rangharajan et al., 2015; Xing et al., 2010; Zheng et al., 2012)
	NBs como agentes carreadores de drogas no combate de células cancerígenas	(Lukianova-Hleb et al., 2014b, 2012)
	NBs como carreadores genéticos	(Cavalli et al., 2015, 2013, 2012)
	Tratamento periodontal com uso de NBs de ozônio	(Hayakumo et al., 2014, 2013)
	Detecção de malária	(Lukianova-Hleb et al., 2014a)
	Prevenção de sufocamento/oxigenação de células sanguíneas	(Kheir et al., 2012)
Sistemas energéticos	NBs de H_2 em gasolina	(Oh et al., 2015)
	Produção de NBs de vapor com energia solar e eficiência energética	(Polman, 2013)
Tratamento de efluentes	Revisão de NBs para tratamento de efluentes	(Agarwal et al., 2011; Gurung et al., 2016)
	Geração de NBs integradas com radiação UV para degradação de surfactantes	(Tasaki et al., 2009a)
	NBs para tratamento biológico aerado	(Kazuyuki et al., 2010)
	NBs na flotação para remoção de poluentes	(Calgaroto et al., 2016)* * Artigo objeto da presente Tese. (Tsai et al., 2007)
	NBs de ozônio na desinfecção de águas e efluentes	(Chen, 2009; Kerfoot, 2015, 2014; Takahashi and Chiba, 2007)
Processamento mineral por flotação	Flotação de partículas de quartzo assistida por NBs	(Calgaroto et al., 2015)* * Artigo objeto da presente Tese.
	Flotação assistida por NBs: mecanismos envolvidos na flotação de minérios e aplicações de NBs no beneficiamento mineral (calcopirita, fosfatos, carvão)	(Ahmadi et al., 2014; Fan et al., 2010a, 2010b, 2010c, 2010d; Sobhy et al., 2013)

Embora a literatura envolvendo nanobolhas tenha se difundido de maneira bastante ampla, ainda são necessárias investigações sobre os procedimentos de geração sustentável (alta

concentração de NBs com eficiência energética) e uma melhor compreensão das propriedades interfaciais e estruturais desses sistemas. Entretanto, poucos são os estudos realizados sobre a estabilidade de nanobolhas dispersas em água, com eletrólitos inertes ou na presença de surfactantes (Jia et al., 2013; Najafi et al., 2007; Takahashi, 2005).

Nos processos de flotação mineral (assistida por NBs) de partículas finas e ultrafinas, por exemplo, estudos aplicados têm demonstrado que as NBs são responsáveis por aumentar ângulos de contato na interface sólido/líquido/ar (minerais de carvão, fosfatos, quartzo e cobre), o que aumenta a probabilidade de flotação devido a uma melhoria no mecanismo de adesão bolha-partícula e na estabilidade desses agregados. Outros benefícios reportados na flotação são o aumento na recuperação de partículas finas de carvão com a utilização de baixas concentrações de reagentes coletores e espumantes e o aumento de cinética de processos (Fan et al., 2012, 2010a, 2010b, 2010c, 2010d; Sobhy et al., 2013; Sobhy, 2013).

Por outro lado, na flotação para remoção de poluentes em águas e efluentes líquidos, a literatura envolvendo NBs ainda é bastante escassa, especialmente no cenário nacional. Recentemente, Etchepare et al. (2016) desenvolveram um estudo sobre o papel das NBs nos processos de FAD para tratamento de águas e efluentes líquidos. Neste contexto, em pesquisas realizadas no LTM/UFRGS, foi descoberto que no processo conhecido como flotação por ar dissolvido (FAD), ocorre a geração conjunta de microbolhas (MBs) e NBs (Calgaroto, 2014; Calgaroto et al., 2014).

1.1 OBJETIVOS

1.1.1 Objetivo Geral

O objetivo geral desta tese é disponibilizar, a partir de estudos básicos de geração, caracterização e aplicação de NBs em sistemas de flotação (áreas mineral e ambiental), uma técnica otimizada de geração de NBs em alta taxa por despressurização, e avaliar os efeitos das NBs na flotação de partículas finas de quartzo (área mineral) e na remoção de aminas em solução aquosa, por precipitação-flotação (área ambiental). As metas técnicas foram a validação do conjunto de métodos e processos propostos, em escala de bancada, e a indicação de parâmetros ótimos de geração de NBs, bem como a transferência do conhecimento gerado por meio de publicações em periódicos científicos internacionais.

1.1.2 Objetivos Específicos

Os objetivos específicos são os seguintes:

- Avaliar os parâmetros pressão de saturação (Psat) e tensão superficial do líquido (Tsup) na geração de NBs por despressurização, avaliando a concentração numérica e o tamanho médio das NBs dispersas em líquido;
- Caracterizar as dispersões aquosas de NBs para os parâmetros potencial zeta, diâmetro médio e concentração de NBs em água deionizada pura e soluções de tensoativos (α-Terpineol e decil-eter-amina);
- Analisar as interações de NBs com bolhas macrométricas e microbolhas, avaliando o tempo de ascensão dessas bolhas na presença e ausência de NBs;
- Analisar as interações de NBs com partículas sólidas e os efeitos do condicionamento de superfícies sólidas de quartzo e pirita na hidrofobização dessas partículas, avaliando o ângulo de contato de adesão de bolhas maiores nessas partículas;
- Avaliar a estabilidade de NBs em dispersão aquosa, analisando o decaimento na concentração de NBs e a sua variação do diâmetro médio ao longo de um período de duas semanas;
- Avaliar a flotação com NBs isoladas (F-NBs) e a FAD na remoção de precipitados coloidais de aminas;
- Avaliar os efeitos do condicionamento com NBs na recuperação de partículas de quartzo em diferentes faixas granulométricas;
- Discutir os mecanismos envolvidos nos sistemas de flotação diversos e propor novos processos de flotação com injeção de NBs, apresentando fluxogramas de processos para aplicações na flotação de minérios e para o tratamento de efluentes líquidos;

1.2 PLANO DE TESE

Esta tese é apresentada na forma de artigos científicos, publicados em periódicos internacionais e está organizada em três partes, cada uma sendo constituída pelos seguintes itens:

Parte I: Introdução, Objetivos geral e específicos e Integração de artigos;

Parte II: Artigos Científicos - Cada artigo científico representa um Capítulo, sendo dividido em, no mínimo: Introdução, Materiais e Métodos, Resultados, Conclusões e Referências Bibliográficas;

Parte III: Considerações finais, Produção Científico-Tecnológica Associada à Tese, Conclusões, Sugestões para trabalhos futuros e Bibliografias;

Os trabalhos elaborados e realizados durante esta tese foram desenvolvidos no Departamento de Engenharia de Minas da UFRGS, no Laboratório de Tecnologia Mineral e Ambiental – LTM.

2. INTEGRAÇÃO DOS ARTIGOS CIENTÍFICOS

A presente tese é um trabalho de P&D&I na linha de pesquisa em geração e caracterização de dispersões aquosas de nanobolhas, avaliando seus comportamentos e efeitos em sistemas bifásicos (ar/líquido) e trifásicos (ar/líquido/sólido) e demonstrando o potencial tecnológico das nanobolhas em sistemas de flotação nas áreas ambiental e mineral.

Os principais avanços e metas técnicas do trabalho foram:

i. O desenvolvimento de uma técnica otimizada de geração de NBs dispersas em água por despressurização, com elevada concentração de bolhas;

ii. Melhor entendimento das interações de NBs com partículas minerais e com outros tipos de bolhas (microbolhas e bolhas milimétricas);

iii. Melhor entendimento das propriedades físicas e interfaciais (potencial zeta e tamanho médio) de NBs dispersas em líquidos, geradas em diferentes condições (pressão de saturação e tensão interfacial do líquido), e da estabilidade das dispersões de NBs em tempos longos;

iv. Desenvolvimento e avaliação em escala de bancada de uma técnica de flotação assistida por NBs para aplicação no setor mineral, utilizando um modelo de partículas de quartzo em diferentes faixas granulométricas;

v. Desenvolvimento e avaliação em escala de bancada de uma técnica de flotação por NBs isoladas para aplicação no tratamento de efluentes, na remoção de precipitados coloidais de aminas;

vi. Transferência do conhecimento adquirido ao setor produtivo, a partir de processo de patenteamento da técnica de geração de NBs, publicações em periódicos e apresentações em congressos nacionais e internacionais;

Estas metas técnicas foram os objetos das publicações internacionais realizadas e a integração destes artigos científicos alcança o objetivo geral proposto para esta tese.

A apresentação dos artigos científicos nessa Tese não obedecerá à ordem cronológica de publicação dos mesmos, uma vez que foram iniciados estudos de aplicações das NBs (flotação de quartzo e de precipitados de aminas) anteriormente aos estudos de otimização da geração de NBs por despressurização e caracterização físico-química das suspensões aquosas de NBs.

Os estudos de geração e caracterização desses sistemas contendo NBs (Artigo I) foram possíveis após a aquisição de equipamento com a técnica *Nanoparticle Tracking Analysis* (NTA, ZetaView®, Particle Metrix, Germany) e foram publicados no periódico *Minerals Engineering* no ano de 2016. O equipamento NTA permite a quantificação das NBs em sistemas líquidos (número de $NBs.mL^{-1}$) e a sua caracterização físico-química com medidas de tamanho e potencial zeta.

Os estudos de aplicação das NBs nos sistemas de flotação propostos, na flotação de partículas de quartzo (Artigo II, *International Journal of Mineral Processing*, 2015) e na flotação de precipitados de aminas (Artigo III, *Minerals Engineering*, 2016), utilizaram-se dos antecedentes técnicos do LTM, quando foi descoberta a geração simultânea de NBs e MBs no processo de FAD convencional, onde ocorre a despressurização, em constritores de fluxo, de uma corrente de água previamente saturada em ar e foi feita uma caracterização físico-química com relação ao tamanho médio e às cargas superficiais das NBs dispersas em água (Calgaroto et al., 2014).

2.1 ARTIGO I – CARACTERIZAÇÃO DE DISPERSÕES AQUOSAS DE NANOBOLHAS

Nesse artigo foi realizado um estudo conceitual acerca dos principais parâmetros envolvidos na geração de NBs (pressão de saturação e tensão interfacial do líquido), avaliando a concentração numérica de NBs por unidade de líquido e seu tamanho médio, buscando atingir uma condição de geração ótima de NBs, com alta concentração e eficiência energética.

O *know-how e o know-why* do LTM nas áreas mineral e ambiental entregam diversos produtos e processos à indústria nacional nestes mais de 30 anos, destaque para as patentes nas áreas de remoção de amônia (PI 0406319-8), recirculação de água de lavagem de veículos (PI 0006390-8) e reator de geração de flocos (PI 0406106-3). Nesta tese, a partir dos resultados alcançados nesses estudos de geração de NBs dispersas em líquido, um pedido de patente foi depositado no Instituto Nacional da Propriedade Industrial (INPI) para processo e equipamento de geração

suspensão aquosa altamente concentrada de NBs (Número processo INPI: BR 10 2016 006081 8), para aplicação em diversos setores produtivos e de serviços.

Neste artigo foi apresentada a primeira microfotografia de uma suspensão aquosa de NBs disponível em literatura, realizada por microscopia ótica (aumento de 1000 X) com auxílio de um corante azul de metileno para possibilitar o contraste entre as fases líquida e gasosa. Ainda, foram realizados estudos da interação de NBs com MBs e com superfícies sólidas hidrofóbicas, utilizando uma partícula mineral de pirita (FeS_2) como modelo e a validação de estudos relativos a estabilidade e longevidade de NBs dispersas em água, com medidas de concentração e tamanho médio de NBs realizadas diariamente por um período de 14 dias. Os resultados são explicados em termos de fenômenos interfaciais e acredita-se que esse artigo possui avanços que possibilitam a ampliação do potencial tecnológico das NBs.

2.2 ARTIGO II – FLOTAÇÃO DE PARTÍCULAS DE QUARTZO ASSISTIDA POR NANOBOLHAS

A descoberta da geração de NBs no processo de FAD como antecedente técnico da pesquisa sobre nanobolhas no LTM (Calgaroto et al., 2014) motivou a investigação dos seus efeitos nos processos de flotação no beneficiamento mineral. A partir de referências de literatura que reportam as vantagens das NBs geradas por cavitação hidrodinâmica, com uso de sistemas compostos de bombas centrífugas e tubos de venturi adaptados (cavitation tube), na recuperação de partículas minerais em processos de flotação em coluna (Ahmadi et al., 2014; Fan et al., 2010a, 2010b, 2010c, 2010d; Sobhy, 2013; Sobhy and Tao, 2013), foi elaborado um estudo em escala de bancada, utilizando partículas de quartzo de diferentes faixas granulométricas como modelo de partículas minerais com o objetivo de investigar os efeitos das NBs geradas pela FAD na recuperação de partículas de quartzo por flotação por ar induzido (FAI) em tubo de Hallimond.

Os ensaios de flotação de bancada demonstraram um aumento significativo da eficiência de flotação de partículas ultrafinas e finas de quartzo, com recuperação de 87% das partículas ultrafinas (D32 = 8 μm) e 85% das partículas finas (D32 = 34 μm), após o condicionamento das partículas com suspensão aquosa de NBs, enquanto a recuperação das partículas ultrafinas e finas sem condicionamento com NBs apresentou valores de 75% e 68%, respectivamente.

Os efeitos positivos das NBs na flotação de finos e ultrafinos foram explicados por mecanismos de agregação e aumento da hidrofobicidade de partículas, comprovados com microfotografias e medidas de ângulo de contato bolha-partícula.

Acredita-se que os resultados desse artigo contribuem para um melhor entendimento dos mecanismos de interação de NBs com partículas minerais e podem abrir novas linhas de pesquisa e levar ao desenvolvimento de produtos tecnológicos na área de flotação de minérios, com alta eficiência de recuperação de partículas minerais finas e ultrafinas e menor consumo de reagentes químicos de flotação, reduzindo o impacto ambiental dos processos da indústria mineral, como uma prática de Produção mais Limpa (P+L).

2.3 ARTIGO III – SEPARAÇÃO DE ESPÉCIES INSOLÚVEIS DE AMINAS POR FLOTAÇÃO COM MICRO E NANOBOLHAS

Neste terceiro artigo científico uma técnica de flotação com NBs isoladas (F-NBs) foi desenvolvida e avaliada em escala de bancada na remoção de amina em efluente aquoso. A precipitação de aminas foi realizada a partir da alcalinização do meio a pH 10,5. Uma caracterização físico-química e morfológica dos precipitados de aminas foi feita, revelando uma ampla distribuição de tamanho, com partículas coloidais com tamanho inferior a 1 μm e partículas maiores com tamanho de até 200 μm. A morfologia dos precipitados e suas interações com NBs foram estudadas com uso de microscopia ótica de alta resolução, demonstrando os efeitos de agregação dos nanoprecipitados e o aprisionamento de NBs na matriz de precipitados micrométricos.

Os estudos de flotação demonstraram que a F-NBs foi mais eficiente na remoção desses precipitados, atingindo eficiência de remoção de até 85% com altas concentrações iniciais de amina (300 $mg.L^{-1}$) após precipitação e floculação com policloreto de alumínio (PAC), enquanto que o uso da FAD convencional apresentou eficiências de remoção entre 50% e 60%. Esses resultados foram explicados devido ao baixo tempo de residência de MBs no sistema de flotação e fragilidade dos precipitados orgânicos, que na presença de MBs e a turbulência causada pelo movimento de ascensão das bolhas pode causar a ruptura desses agregados, diminuindo assim a probabilidade adesão e flotação dos mesmoss. As NBs, por sua vez, apresentam forte interação com espécies hidrofóbicas e sua alta estabilidade em meio líquido faz com que interajam com os precipitados de amina, reduzindo a densidade dos mesmos e promovendo a sua separação por flotação.

Os resultados desse artigo são um ponto de partida para linhas de pesquisa na aplicação de F-NBs na remoção de poluentes em efluentes aquosos. A pesquisa com NBs na remoção de poluentes segue no LTM com investigação dessa técnica desenvolvida na remoção de precipitados inorgânicos (co-precipitados de sulfato-alumínio e hidróxidos de ferro e cobre) e poluentes orgânicos, na floculação-flotação de efluentes oleosos.

PARTE II

AQUEOUS DISPERSIONS OF NANOBUBBLES: GENERATION, PROPERTIES AND FEATURES

Artigo publicado no periódico Minerals Engineering, volume 94, 2016, páginas 29–37.

3. AQUEOUS DISPERSIONS OF NANOBUBBLES: GENERATION, PROPERTIES AND FEATURES

Azevedo, A., Etchepare, R., Calgaroto, S., *Rubio, J.

Laboratório de Tecnologia Mineral e Ambiental, Departamento de Engenharia de Minas, PPGE3M, Universidade Federal do Rio Grande do Sul, Av. Bento Gonçalves, 9500, Prédio 43427 - Setor 4, CEP: 91501-970, Porto Alegre, RS, Brazil, www.ufrgs.br/ltm,
*Corresponding author: jrubio@ufrgs.br

ABSTRACT

Nanobubbles (NBs) have interesting and peculiar properties such as high stability, longevity and high surface area per volume, leading to important applications in mining-metallurgy and environmental areas. NBs are also of interest in interfacial phenomena studies involving long-range hydrophobic attraction, microfluidics, and adsorption at hydrophobic surfaces. However, little data are available on effective generation of concentrated NBs water dispersions and on their physicochemical and interfacial properties. In this work, air was dissolved into water at pH 7 and different pressures, and a flow was depressurized through a needle valve to generate 150-200 nm (mean diameter) NBs and MBs-microbubbles (about 70 μm). Microphotographs of the NBs were taken only in the presence of blue methylene dye as the contrast medium. Main results showed that a high concentration of NBs (number per volume) was obtained by decreasing the saturation pressure and surface tension. The number of NBs, at 2.5 bar, increased from 1.0 x 10^8 NB.mL^{-1} at 72.5 mN.m^{-1} to 1.6 x 10^9 NB.mL^{-1} at 49 mN.m^{-1} (100 mg.L^{-1} α-Terpineol). The NBs mean diameter and concentration only slightly varied within 14 days, which demonstrates the high stability of these highly concentrated NBs aqueous dispersions. Finally, after the NBs were attached to the surface of a grain of pyrite (fairly hydrophobic mineral), the NBs dramatically increased the population of MBs, which shows the enhancement of particle hydrophobicity due to NBs adhesion. The results were explained in terms of interfacial phenomena and it is believed that these tiny bubbles, dispersed in water at high concentrations, will lead to cleaner and more sustainable mineral flotation.

Key words: Nanobubbles generation, stability, interfacial properties, mineral flotation

3.1 INTRODUCTION

Nanobubbles (NBs[1]) occur as highly stable adsorbed units (interfacial or surface NBs) and spread out as either pancake-like structures or liquid dispersions (bulk NBs). The first report of interfacial NBs is an experimental work that measured the attractive force among hydrophobic surfaces immersed in water (Parker et al., 1994). Accordingly, this behavior is a step-like function of the separation distance among the surfaces, which is ascribed to the presence of submicron bubbles that connect the surfaces. Thereafter, experimental evidence of NBs was provided by Miller et al. (1999), who used Fourier transform infrared (FTIR) spectroscopy to investigate the n-butane-saturated water at a hydrophobic silicon solid. These measurements revealed the accommodation of butane gas by interfacial water at hydrophobic surfaces, supporting the actual presence of NBs.

NBs are gaseous domains that are typically tens to hundreds of nanometers in radius, which are too small to be visible to the naked eye or standard microscopes. Atomic Force Microscope (AFM) images revealed that they form spherical caps, but the precise shape of the NBs remains unclear (An et al., 2015). Today, surface NBs (present in aqueous submerged hydrophobic surfaces) can be detected using different microscopy techniques, most notably tapping-mode AFM (Hampton and Nguyen, 2009; Lou et al., 2000). Chan and Ohl (2012) and Karpitschka et al. (2012) used total internal reflection fluorescence microscopy (TIRFM) for images of hydrophobized glass plate surfaces with adhered NBs.

Bulk NBs are believed to be long-lived gas-containing cavities affected by random Brownian motion. It is now thought that bulk NBs are present in water at room temperature because of the nucleation of stable bubbles. Thus, there is a water affinity property at the nanoscale, whereby the disordered structure of a liquid becomes unstable and results in a spontaneous decrease in local density and formation of nano-sized voids. These voids would serve as nuclei for bubbles that are stabilized by ions (so-called bubstones) (Bunkin et al., 2012). These bulk NBs have been detected using different techniques such as light scattering, resonant mass

[1] Footnote: In this work, NBs are defined as bubbles that are less than a micron in size (sub-micron bubbles), although the term “nano” is applied mostly to sizes of approximately 1-100 nm (ISO/TS 27687:2008).

measurement and a ZetaSizer Nano instrument, which uses Laser Doppler Micro-electrophoresis.

The main properties of NBs are their high stability, longevity and rapid attachment to hydrophobic surfaces. These particularities broaden the potential applications of NBs in many areas such as surface coating and cleaning (Liu et al., 2008; Liu and Craig, 2009; Ushida et al., 2012b; Wu et al., 2008; Yang and Duisterwinkel, 2011b), pollutant removal (Agarwal et al., 2011; Fraim and Jakhete, 2015; Kazuyuki et al., 2010; Kerfoot, 2015, 2014; Li et al., 2014; Tasaki et al., 2009b; Tsai et al., 2007), energy system improvement (Chan et al., 2015; Hou et al., 2015; Oh et al., 2015; Polman, 2013), medicine (Cavalli et al., 2015, 2013, 2012, Lukianova-Hleb et al., 2014a, 2014b, 2012; Reshani H Perera et al., 2014), fluidics (Hampton and Nguyen, 2010; Ushida et al., 2012a; Zhang et al., 2006; Zimmerman et al., 2011), and agricultural and acceleration of metabolism in vegetable/animal species (Ebina et al., 2013; Liu et al., 2013; Takahashi and Chiba, 2007).

In the mineral flotation of fine and ultrafine particles, NBs were found to increase the contact angles (coal, phosphates, quartz, and copper minerals), which improves the particle-bubble attachment and decreases the detachment. Other claimed flotation gains are a lower collector and frother dosages required in high kinetic processes (Fan et al., 2012; Sobhy and Tao, 2013a; Sobhy and Tao, 2013b; Sobhy, 2013). In addition, in the environmental area, technologies involving NBs have been applied in the removal of amine collector (Calgaroto et al., 2016); bioremediation of groundwater, degradation of surfactants and industrial wastewater treatment (Agarwal et al., 2011; Fraim and Jakhete, 2015; Kazuyuki et al., 2010; Kerfoot, 2015, 2014; Li et al., 2014; Tasaki et al., 2009b; Tsai et al., 2007).

Further research involving interfacial and bulk NBs are important to understand the fundamentals and broaden their technological applications. There is a demand for advances in terms of sustainable (workable) generation, mineral particles aggregation, hydrophobizing power and flotation (minerals fines and wastewater treatment and reuse).

In the dissolved air flotation (DAF) process, stable (charged or uncharged) NBs are readily formed after the depressurization of air-saturated water at a high flow velocity, and a known distribution size of NBs can be obtained by either modifying the pH or introducing ionic surfactants (collector-coated NBs). This joint formation of microbubbles (MBs) and NBs was proven notably recently, and a separation technique in which NBs are split from MBs is now available (Calgaroto et al., 2015, 2016).

According to many authors, the extremely high stability and longevity of bulk NBs cannot be explained uniquely by the surface potential and repulsion forces between the bubbles (Craig, 2004; Hampton and Nguyen, 2010; Lima et al., 2008; Ohgaki et al., 2010; Seddon et al., 2011; Weijs and Lohse, 2013). The DLVO theory generally works well under the circumstances for which it was originally intended, i.e., low salt, inert surfaces and interactions at separations greater than a few nanometers. The long-ranged attractions, which are measurable up to several hundred nanometers, among hydrophobic NBs do not fit in this theory. Thus, unfortunately, calculations are difficult to make due to the fact that the forces presumably operate in this size range of the NBs. Further research is required, and many challenges remain (Calgaroto et al., 2014).

This study is a continuation of a series of articles regarding NBs and focuses on their generation as highly loaded aqueous dispersions, characterization, interfacial properties, lifetime and their role in hydrophobizing mineral solids.

3.2 EXPERIMENTAL

3.2.1 Materials

Deionized (DI) water at room temperature (23°C ± 1) with a conductivity of 3 $\mu S.cm^{-1}$, a surface tension of 72.5 ± 0.1 $mN.m^{-1}$ and a natural equilibrium pH of 5.5 was used to produce NBs aqueous dispersions. The DI water was prepared from tap water using a purification system, which consisted of a reverse-osmosis cartridge and modules of ion-exchange resins and activated carbon. A sulfochromic solution and subsequent abundant rinse with DI water were used to remove possible organic compounds from all glass materials. NaCl, which was supplied by Synth® (São Paulo - SP, Brazil) was used to prepare the saline solutions for NBs characterization; NaOH and HCl solutions from Vetec® (Rio de Janeiro - RJ, Brazil) were used for medium pH adjustments.

Methylene blue from Sigma® (St. Louis - MO, USA) was used as a contrast medium to take microphotographs of the NBs.

α-Terpineol (supplied by Química Maragno®; Turvo – SC, Brazil) was used to reduce the water surface tension and NBs generation. This reagent is a 154 $g.gmol^{-1}$ molecular weight commercial terpene alcohol with the following molecular formula: $CH_3 – C_6H_9 – (OH) – C_3H_5$.

3.2.2 Methods

NBs aqueous dispersion generation

Bubbles were formed by reducing the pressure of DI water, which was pre-saturated with air at various saturation pressures (P_{sat}) during 30 min. This method followed a technique described by Calgaroto et al. (2014), where the supersaturated water was forced through a needle valve (2 mm internal diameter: Globo 012 - Santi®, São Paulo – SP, Brazil), and MBs and NBs were generated in a glass column. The saturation of air in DI water was achieved in a stainless-steel vessel, which contained an internal glass container; the vessel had a height of 15 cm, an inner diameter of 12 cm, and a wall thickness of 1 cm. The container had a height of 14 cm, an inner diameter of 10 cm, a wall thickness of 0.5 cm, and a capacity of 0.7 L.

Then, the MBs were separated from the NBs because the MBs were allowed to rise and escape the glass column (during 5 min), as in Calgaroto et al. (2015). This procedure, which is illustrated in Fig. 3.1, takes advantages of the high stability of NBs in aqueous systems and their lack of buoyancy (Attard, 2003; Gray-Weale and Beattie, 2009; Hampton and Nguyen, 2010; Ohgaki et al., 2010; Seddon et al., 2011; Weijs and Lohse, 2013).

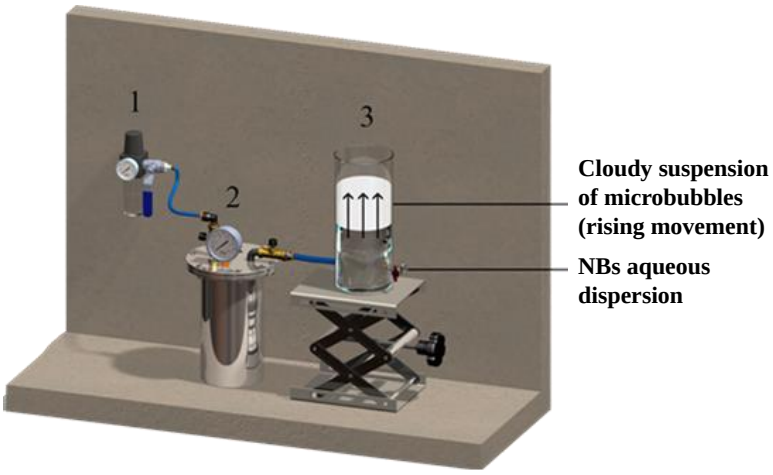

Figure 3.1. Experimental set-up to generate bubbles and separate the MBs from the NBs. (1) Compressed air filter; (2) Saturator vessel coupled to a needle valve; (3) Glass column.

Optical microscopy: image analysis of bulk NBs

Optical microphotographs of bulk NBs were taken using an optical microscope (Olympus®, Hicksville – NY, USA; model BX41) with backlight and an objective magnification of 1000x, which was coupled to a Microscope Digital Camera of high-performance (Olympus® DP73 - 17.28 megapixel of resolution). Methylene blue dye (about 50 mg) was added and mixed into

100 mL of NBs aqueous dispersion to enhance the contrast of the images. One drop of this sample was placed between the microscope slide and the cover slip. Then, both were inserted in the microscope for viewing. The image analysis software ImageJ® (Bethesda – MD, USA) was used to determine the mean diameter of the NBs in these images.

Size, concentration and zeta potential measurements of NBs

The concentration, mean size and size distribution of the NBs were measured in quadruplicates in a nanoparticle-tracking analysis (NTA) instrument (NanoSight LM10 & NTA 2.0 Analytical Software, Malvern Instrument Ltd, Salisbury, UK) at room temperature. The NTA was equipped with a cell (model LM10) and a 20x magnification microscope, onto which a video camera was mounted. The camera captured a video file of the particles, which moved in Brownian motion, and the software tracked the particles individually. Then, using the Stokes-Einstein equation, the hydrodynamic diameter of NBs was calculated. The video images of the particles light scattered were followed in real-time using a CCD camera. The NBs aqueous dispersion samples (approximately 0.1 mL) were injected into the cell with sterile syringes (5 mL of capacity) until the liquid reached the tip of the nozzle. All samples were measured without dissolution, and each video clip was captured during 10 seconds with a manual shutter and gain adjustments. The NTA analytical software was used for capture and calculations. The obtained values of the mean size, size distribution and number of NBs are the arithmetically calculated values for a triplicate experiment.

The advantage of this technique is that the NTA monitors the light scattered by individual nanoparticles (NBs in this case). Furthermore, because of the particle-by-particle measurement basis, the NTA can characterize polydisperse particulate systems with high precision (Filipe et al., 2010).

A ZetaSizer Nano ZS (red badge) - ZEN3600 (Malvern Instrument Ltd, Salisbury, UK), which was coupled to disposable folded capillary cells (gold-plated Beryllium Copper electrodes), measured the zeta potential, and mean size of the NBs. This instrument uses a Laser Doppler Micro-electrophoresis technique, where an electric field is applied to the dispersion of bubbles that migrate at a velocity that depends on the zeta potential. This velocity is measured using laser interferometry-M3-PALS (phase analysis light scattering), which enables the calculation of electrophoretic mobilities and converts them into a zeta potential (millivolts) using Smoluchowski´s equation (Hunter, 1981).

To measure the mean size of the NBs, the ZEN3600 uses a dynamic light-scattering (DLS) technique, which monitors the diffusion of the bubbles that move in Brownian motion and converts this signal to equivalent diameters according to the Stokes–Einstein relationship. The high sensitivity of this equipment was ensured using a non-invasive backscatter technology.

The zeta potential and size were measured at a scattering angle of 90°, a wavelength of 290 nm and a temperature of 296 K. Each obtained zeta potential and size measurement corresponded to the mean values of 90 measurements (45 for two different samples). The mean values and standard deviation of the zeta potentials were calculated by assuming an average distribution of the generated data (1-5% for the zeta potential values and 2-20% for the bubble size results).

Effect of P_{sat} and water surface tension on the NBs concentration

The concentration and size distribution of the NBs were assessed with NTA in quintuplicates using different P_{sat} values (2.5-6 bar) in the generation procedure of NBs aqueous dispersion (described in 2.2.1) at various surface tension values. The surface tension of the water changed with F507 (50 $mg.L^{-1}$) and α-Terpineol solutions at different concentrations (100, 70, 50, 20, and 10 $mg.L^{-1}$); the NBs dispersions were produced using these solutions. The surface tension of the solutions was measured using a Kruss® (Hamburg, Germany) model 8451 tensiometer (resolution of 0.1 $mN.m^{-1}$). Three readings were made for each sample to determine any change with time before obtaining averaged values.

NBs aqueous dispersion properties

i. Bubble stability and longevity as functions of time.

NBs aqueous dispersions were generated in two different solutions (i. DI water; ii. α-Terpineol solution - 100 $mg.L^{-1}$) according to the aforementioned method with a P_{sat} of 2.5 bar and pH of 7. The bubble size distribution and concentration of NBs were subsequently measured as a function of storage time (during 14 days) using NTA. Both NBs aqueous dispersions (200 mL) were maintained in covered glass beakers and stored in the dark in a styrofoam box at a constant temperature of 21°C. The measurements for each sample (0.1 mL approximately) were performed in quadruplicates.

ii. Zeta potential of NBs in α-Terpineol solutions

NBs were generated in 10^{-3} M NaCl solutions at a P_{sat} of 2.5 bar. The pH effect on their zeta potential and mean size (both measured using the ZEN3600) was assessed in duplicate experiments.

iii. Rising velocity of bubbles

The effect of NBs on the rising velocity of MBs was investigated (in duplicate experiments - error ± 10%) in a glass column cell (height = 21 cm; diameter = 10 cm). Air-saturated water (0.3 L, P_{sat} = 5 bar) was forced through the same needle valve (2.2.1) into the bottom of the glass cell, which contained 1 L of NBs aqueous dispersion. Then, the time for the cloud of bubbles to rise the distance from the bottom of the column to the liquid surface, was measured using a chronometer. The rising velocities of MBs were investigated for bubbles that were generated in DI water (pH 7) and with α-Terpineol solution (100 $mg.L^{-1}$; pH 7). The blank experiments were performed with the cell that contained either DI water or α-Terpineol solutions without NBs.

iv. Adhesion of bubbles at the pyrite/water interface

The effect of NBs conditioning on the MBs attachment onto hydrophobized solid particles was investigated using a 2 mm grain size pyrite as a fairly hydrophobic particle model. The NBs aqueous dispersion was made using 100 $mg.L^{-1}$ α-Terpineol solution and by directly depressurizing (P_{sat} = 2.5 bar) into a glass beaker with subsequent separation of MBs as described by Calgaroto et al. (2015). The experimental setup (Fig. 3.2) consisted of the stainless-steel saturator vessel, which was coupled to a needle valve for micro and NBs generation (2.2.1), a flat glass cell and a stereomicroscope Zeiss® (Oberkochen, Germany) Stemi SV11, which was coupled to a digital camera (Sony NEX-3).

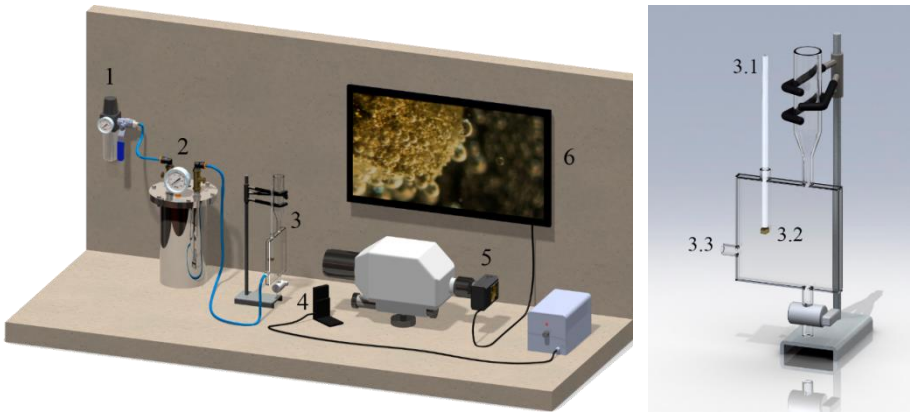

Figure 3.2. Experimental set-up for image acquisition of the MBs-pyrite interaction in the absence and presence of NBs. Left side: (1) Compressed-air filter; (2) Saturator vessel; (3) Flat glass cell; (4) White-light source; (5) Stereomicroscope coupled to a digital camera; (6) Monitor for image reproduction. Right side: Details of the flat glass cell. (3.1) Pyrite grain holder; (3.2) Pyrite grain; (3.3) Cell inlet (for bubbles injection).

First, the pyrite particle was cleaned with a sulfochromic solution to remove possible organic contamination. Then, microphotographs of the pyrite grain, which was placed (fixed) in a glass cell, after the MBs injection, were taken under three conditions: i. Pyrite immersed in DI water; ii. Pyrite immersed in α-Terpineol solution (100 $mg.L^{-1}$) for 5 min before the MBs injection; iii. Pyrite immersed in NBs aqueous dispersion for 5 min before the MBs injection. These experiments were performed in duplicate, and at least six microphotographs were taken for each condition, which showed the MBs adhered to the pyrite surface.

3.3 DISCUSSION

3.3.1 Factors involved in the NBs generation

Microphotographs of uniformly aqueous-dispersed NBs using high-resolution optical microscopy were possible only after contrasting the air-liquid interface with methylene blue dye (Fig. 3.3). The mean diameter of these NBs, which was measured using ImageJ®, was approximately 530 nm.

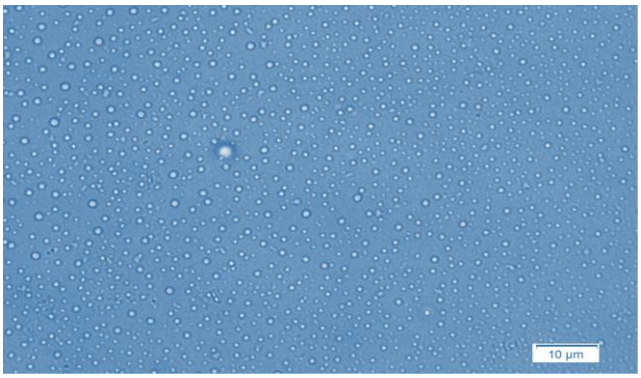

Figure 3.3. Photomicrograph of aqueous-dispersed NBs with methylene blue dye for contrast (NBs and the continuous phase). Conditions: Magnification of 1000 x; NBs generated at pH = 7 and Psat = 2.5 bar.

Information on the visualization of bulk-phase NBs using optical microscopy is scarce, if available. Taking microphotographs of NBs is not easy because of the transparency drawbacks and the necessity of a soluble contrasting medium in the continuous phase. Herein, microphotographs were taken in the presence of methylene blue dye (the bulk NBs do not absorb the dye); the NBs images were neat and highly uniform (homogeneous), which enables the measurement of the NBs mean diameter using the image analysis software ImageJ®. It is believed that these microphotographs are the first optical capture of stable dispersed NBs and certainly will broaden the routes for further characterization studies.

Three different techniques for NBs size measurement were used in this work: i. NTA; ii. DLS and iii. Image Analysis (software ImageJ®). In the measurements with DLS technique, that uses the intensity of light scattered by the sample, the larger NBs (about 300 nm or larger) interfere and "hide" the smaller NBs, giving results of mean diameter higher (300-400 nm) than those obtained by NTA (150-200 nm) for the same NBs generation conditions applied herein (pH 7; P_{sat} = 2.5 bar). The NTA technique monitors the Brownian motion of the NBs and uses the Stokes-Einstein relation to calculate the individual size of each NB in the optical field of the equipment (Malvern, 2014). On the other hand, Image Analysis was only employed to measure the mean diameter of NBs from the microphotographs obtained with optical microscope. Such a technique has the limitation of the microscope used in this study, which does not visualize NBs smaller than 300 nm (diameter).

Another and perhaps the most important contribution of this work is the effect of P_{sat} on the generation and concentration of NBs at two different surface tension values: 49 $mN.m^{-1}$ with 100 $mg.L^{-1}$ of α-Terpineol and 72.5 $mN.m^{-1}$ with DI water (results shown in Fig. 3.4). Surprisingly, at low P_{sat} values (< 3 bar), when the amount of dissolved air in water is too low, the number of generated NBs steadily increases, particularly at low air/water interfacial tension. Under these conditions, a substantial decrease in the cloud of MBs (30-100 μm) was visually observed. The concentration of MBs formed down-stream of the flow constriction is a direct function of the amount of dissolved air in water and increases with increasing P_{sat}, when more air is available (Rodrigues and Rubio, 2007). Then, because the concentration of generated MBs at P_{sat} < 3 bar was notably low, their interaction with the bulk-phase NBs was significantly reduced, and the NBs concentration increased (Fig. 3.4).

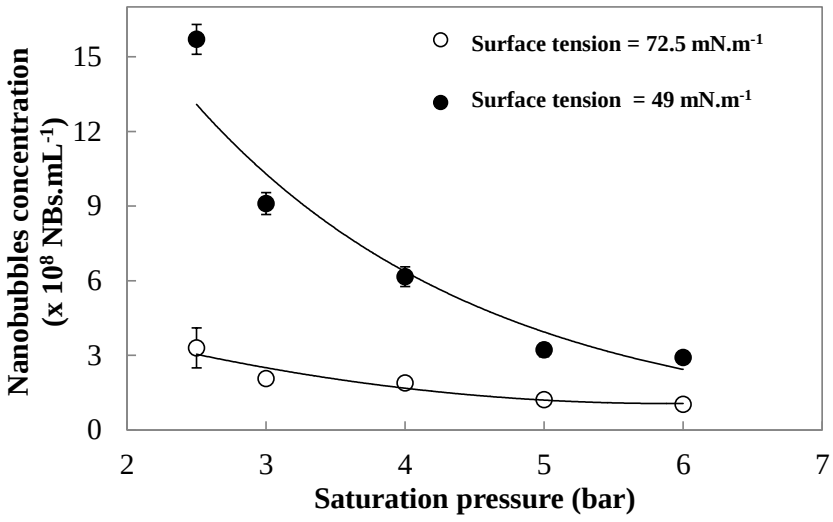

Figure 3.4. NBs concentration (density) as a function of saturation pressure at two aqueous surface tension values. Conditions: pH = 7; surface tension of 49 $mN.m^{-1}$ obtained using 100 $mg.L^{-1}$ α-Terpineol; surface tension of 72.5 $mN.m^{-1}$ obtained using DI water. Measurements were performed with the NTA technique.

Fig. 3.5 shows that the NBs concentration increased by approximately 5 times from 3 x 10^8 $NBs.mL^{-1}$ to 1.6 x 10^9 $NBs.mL^{-1}$ upon a decrease in water/air interfacial tension from 72.4 $mN.m^{-1}$ to 49 mNm^{-1} obtained using 100 $mg.L^{-1}$ α-Terpineol at P_{sat} of 2.5 bar. This phenomenon is similar to that observed in the generation of MBs (Rodrigues and Rubio, 2003) and leads us to the studies of Takahashi et al. (1979) on the minimum "energy" ΔF required for bubble formation (equation 1),

$$\Delta F = \frac{16\pi\gamma^3}{3(P_{sat}-P_o)^2} \qquad (1)$$

where γ is the surface tension of the liquid, and P_o is the atmospheric pressure.

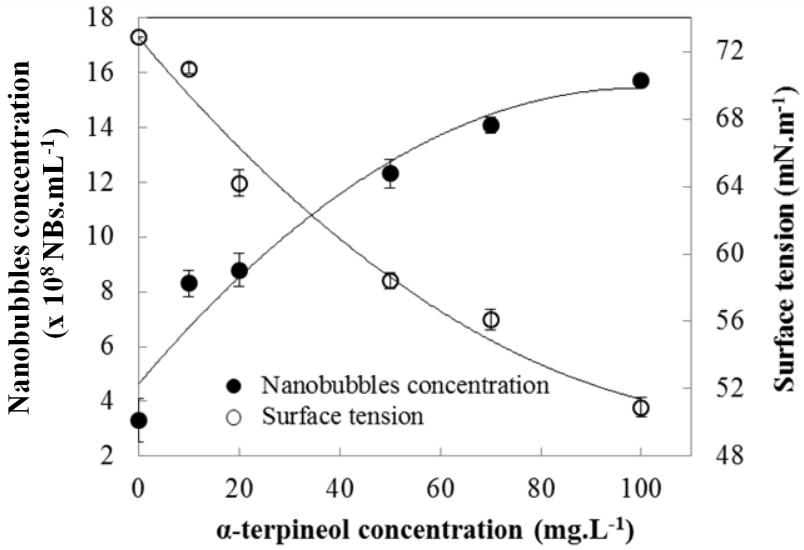

Figure 3.5. Effect of the surface tension (adjusted with α-Terpineol) on the concentration of NBs. Conditions: pH 7; P_{sat} = 2.5 bar. Measurements were performed with the NTA technique.

Accordingly, a certain amount of energy must be transferred to the liquid phase to form bubbles by a cavity phenomenon. Decreasing the air/liquid interfacial tension lessens the liquid/solid attrition, enhances the flow fluid velocity and increases the kinetics of bubble formation (precipitation and nucleation) at the flow constrictor. In practice, the quantity of MBs that form at a P_{sat} of 3 bar or less is notably small; thus, DAF units always operate at pressures above 3 bar (Féris and Rubio, 1999; Rodrigues and Rubio, 2007).

Therefore, the aqueous bulk-phase NBs concentration is a result of several simultaneous events with various equilibria. After the formation in the flow constrictors, the NBs and MBs interact as follows: i. The NBs and MBs collide and attach to each other; ii. The NBs slide around the MBs slip plane; iii. The MBs eventually trap or entrain the NBs. Consequently, some NBs disappear because they are engulfed by the MBs.

Table 3.1 presents data on the up-rising velocity of MBs generated in DI water and/or α-Terpineol solution in mixtures with NBs immediately after the formation of both types of bubbles upon depressurization. This table shows that the velocities of the MBs increased in the presence of an "extra" aqueous bulk-phase, which demonstrates an interaction among the bubbles and a probable coalescence and growth of the MBs by entrapping the NBs. The new and larger MBs-NBs "assemblages" had faster velocities (32-37% higher) in water than in the absence of extra NBs, due to their higher buoyancy.

Table 3.1. Rising velocities of Microbubbles-MBs in deionized (DI) water or α-Terpineol with and without NBs. Conditions: Liquid height in the cell = 21 cm; NBs generation: pH 7; P_{sat} = 2.5 bar; V (solution) = 1 L; MBs generation: P_{sat} = 5 bar, pH = 7, V (of air-saturated water injected into the solution) = 0.3 L.

	DI water			**α-Terpineol solution (100 mg.L^{-1})**		
	Rising time, s	**Rising velocity, cm.s^{-1}**	**Standard deviation, cm.s^{-1}**	**Rising time, s**	**Rising velocity, cm.s^{-1}**	**Standard deviation, cm.s^{-1}**
Without nanobubbles	342	0.062	0.004	358	0.059	0.007
With nanobubbles	261	0.081	0.003	259	0.081	0.006

More, similar to the data obtained at different P_{sat} values, the NBs mean diameters were practically identical (150-200 nm) at all conditions with a narrow size distribution (50-300 nm). Under optimal conditions (a P_{sat} of 2.5 bar and air/aqueous interfacial tension of 49 mN.m^{-1}), the NBs density was high (> 10^9 bubbles.mL^{-1}), the size distribution was notably narrow (50-300 nm), and the superficial area was approximately 730 cm^2.L^{-1} (calculated for spherical NBs considering their mean diameter and concentration). The MBs mean diameter generated by depressurization of air-saturated water was already measured by different methods, especially

by image analyses (Rodrigues and Rubio, 2003), and were found to be in the range of 30-100 μm.

Unfortunately, few data on the concentration of NBs, generated by the different techniques, are available. There are studies reporting the following values: i. 1.97 x 10^8 NBs.mL^{-1} (Liu et al., 2013); ii. 2.8 x 10^8 hydrogen NBs.mL^{-1} (Oh et al., 2015); and iii. 1.9 x 10^{13} NBs.mL^{-1} (Ohgaki et al., 2010). However, in Liu et al.'s (2013) work, the generation method of NBs was not entirely detailed while Oh et al. (2015) used a gas–liquid dispersion system (membrane module). Ohgaki et al. (2010) used a centrifugal multiphasic pump under high pressure (6 bar). In this study, the concentration of NBs was estimated using scanning electron microscopy and the physical properties of the gases, but the size distribution of NBs was not considered, an indirect and not notably accurate procedure which might lead to erratic numbers.

A major gain of the NBs formation technique developed in this work is that it takes advantage of a well-known industrial process DAF; the air depressurization in flow constrictors is widely applied in this technology. Because of the working P_{sat} (> 4 bar), whereby most bubbles are MBs, this process is also named as microbubble flotation. More, most researchers and engineers have not measured neither have been acquainted with the generation of NBs by the DAF process. The use of NTA technique to determine the actual presence of NBs and their concentration as a function of P_{sat} is a major contribution of this work. It is now known that the use of a low P_{sat} (2.5 bar) is a sustainable manner to create dense bulk-phase NBs, at high rates, with low operating costs, energy savings and simplicity.

Summarizing, it seems that it is now possible to obtain highly concentrated (number of NBs per volume) charged or uncharged NBs dispersions with different sizes, with or without adsorbed surfactants (ionic or not) (Calgaroto et al., 2014). The next step is to discover useful applications in flotation by generating NBs (coated or not) in a rapid manner, and ultra-concentrated NBs with a higher degree of uniformity.

3.3.2 Interfacial and stability properties of NBs

Fig. 3.6 shows the effect of pH on the NBs size (mean diameter) and zeta potential, measured using the DLS technique. The NBs became smaller and more electronegative when the medium pH changed from 3 to 8; the mean diameter halved from 500 to 250 nm, and the zeta potential decreased by approximately 40 mv units. This effect was assessed at P_{sat} 2.5 bar and in the presence of α-Terpineol, when a higher population of NBs was obtained. These findings

confirmed earlier results (Calgaroto et al., 2014) that showed that both zeta potential and mean size diameters are pH dependent, at least at pH 3-8. Thus, with the increase in pH, the negative zeta potential of the bubbles increases and the NBs become smaller and highly charged. Presumably, the developed double layer plays an important role in the formation and stability of bulk NBs by providing a repulsive force, which prevents inter-bubble aggregation and coalescence of stable bubbles (Hampton and Nguyen, 2010; Ushikubo et al., 2010).

In addition, NBs are reportedly highly stable with considerable longevity when they are adsorbed onto hydrophobic surfaces (Chan et al., 2015; Peng et al., 2014; Weijs and Lohse, 2013; Zhang et al., 2013) or in the form of aqueous or organic bulk-phase dispersions (Liu et al., 2013). Bulk-phase NBs have drawn widespread research interest; despite various theories and theoretical models that have been proposed to explain their long lifetimes the underlying mechanisms remain in dispute (Hampton and Nguyen, 2010; Peng et al., 2015; Seddon et al., 2011).

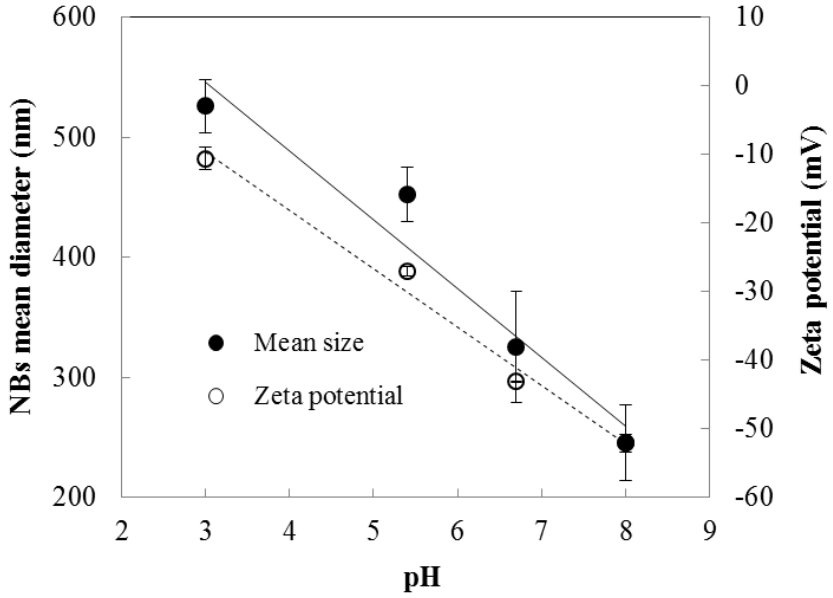

Figure 3.6. Mean diameter and zeta potential of NBs as a function of pH. Conditions: P_{sat} = 2.5 bar; 100 mg.L^{-1} α-Terpineol; surface tension = 49 mN.m^{-1}; [NaCl] = 10^{-3} M. Measurements were performed with the DLS technique.

Fig. 3.7 and 3.8 show data on the evolution of the NBs mean diameter and concentration over 14 days. The results revealed (proved) the high stability and longevity of these bubbles when dispersed in water. The data show a few differences in size and number of NBs during the storage period; the values were always within the SD: 40 nm for mean diameter and 5 x 10^{7} NBs.mL^{-1} for the concentrations. This result is consistent with results of other authors, showing

that NBs can be stable for days or even months (Oh et al., 2015; Ohgaki et al., 2010; Ushikubo et al., 2010).

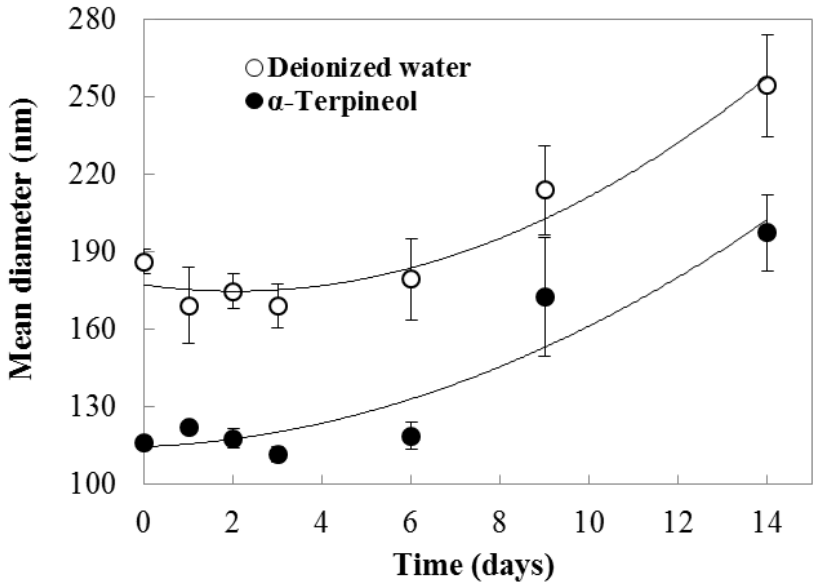

Figure 3.7. Stability of aqueous dispersion of NBs: Mean bubbles diameter as a function of storage time (life time). Point 0.0 in the abscissa refers to the test (obtained size) 10 min after the NBs generation. Conditions: pH 7; P_{sat} = 2.5 bar; [α-Terpineol] = 100 mg.L^{-1} (surface tension = 49 mN.m^{-1}); Deionized water (surface tension = 72.5 mN.m^{-1}). Measurements were performed with the NTA technique.

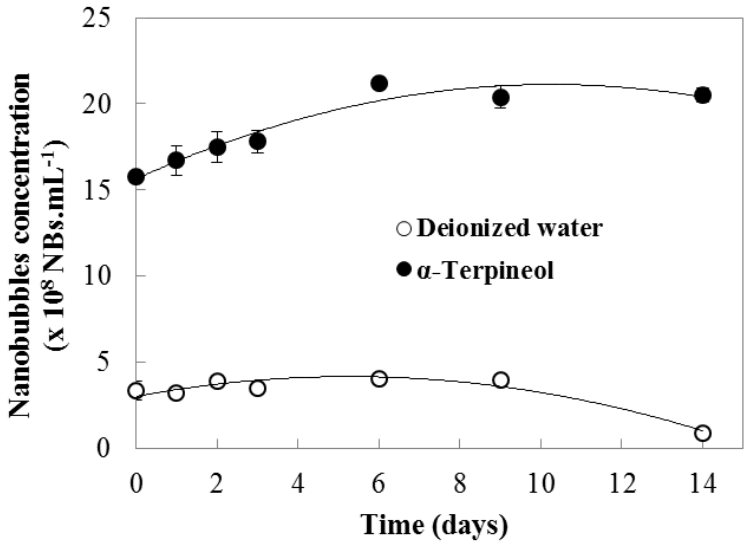

Figure 3.8. Stability of aqueous dispersion of NBs: Bubbles concentration as a function of storage time (life time). Conditions: pH 7; P_{sat} = 2.5 bar; [α-Terpineol] = 100 mg.L^{-1} (surface tension = 49 mN.m^{-1}); Deionized water (surface tension = 72.5 mN.m^{-1}). Measurements were performed with the NTA technique.

In saturated liquids (free from micro-solids), such as in this work, the spontaneous nucleation of dissolved gases leads to NBs formation, and the NBs are notably stable probably because of the following phenomena (among others): i. The gas molecules inside the NBs do not contact the bulk liquid; ii. The gas molecules on the surface of the bubble leaves the surface in a perpendicular direction, and the gas molecules continuously leave and enter in constant flux; iii. The gas molecules usually move from one side of the bubble to the other side without touching one another because of the fineness of the NBs. This movement allows free flow of the liquid along the bubbles, which pushes the gas molecules to the surface of the bubbles and increases their stability; iv. The adsorption of ions on the NBs surface. Negatively charged bubbles adsorb protons onto their surface and result in Coulomb-repulsion forces that compensate the surface-tension forces (Bunkin et al., 2009, 2007; Chaplin, 2007). The ions probably modify the hydrogen-bonding network in water and around the bubble surface, which may enhance the viscosity of water at the bubble/water interface and decrease the mobility of water molecules.

The stability and high surface area per volume are important and useful properties of NBs. Advances in the understanding of NBs in water or complex aqueous solutions may broaden their applications in flotation (minerals and residual flotation reagents residual).

Fig. 3.9 shows photographs of the differential attachment of MBs and their mixtures with NBs at the pyrite/water interface. Only few MBs attached to the pyrite surface (a rather hydrophobic mineral) in the presence and absence of α-Terpineol (better with this “frother”). Conversely, the population of MBs dramatically increased after the pyrite surface was conditioned with NBs. These results validate our data and other authors’ data on the preference of NBs for hydrophobic minerals and moieties (Calgaroto et al., 2015; Chan et al., 2015; Peng et al., 2014; Zhang et al., 2013).

The MBs significantly attached onto the NB-coated pyrite, which proves that the NBs may act as a secondary flotation collector, as previously reported by Fan et al. (Fan et al., 2013, 2012, 2010a, 2010c, 2010d; Fan and Tao, 2008). This phenomenon appears to occur through the hydrophobic interaction between NBs and pyrite: the NBs collide, attach, then aggregate or cluster serving as a hydrophobic layer where other bubbles (MBs or macrobubbles) will adhere.

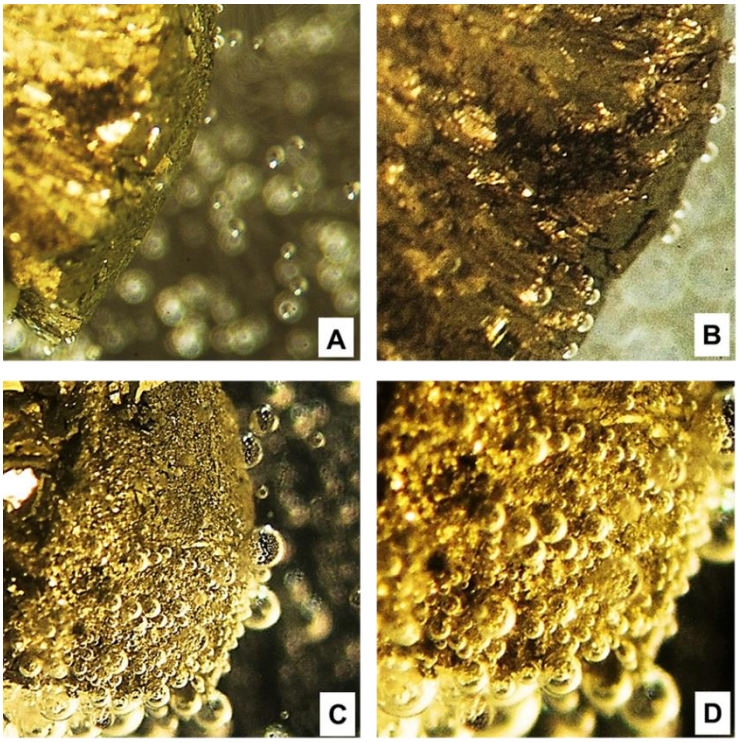

Figure 3.9. Microphotographs of bubble-pyrite particle interactions: A) Pyrite and MBs in DI water; B) Pyrite and MBs in 100 mg.L^{-1} α-Terpineol solution; C) Pyrite and MBs in NBs aqueous dispersion; D) A zoomed-in image of C. Conditions: MBs formed in DI water at pH 7 and P_{sat} = 5 bar. NBs formed with 100 mg.L^{-1} α-Terpineol at pH 7 and P_{sat} = 2.5 bar. Microphotographs taken by a stereomicroscope.

It is expected that the injection of these highly loaded NBs aqueous dispersions in flotation cells or conditioners will improve the overall flotation of minerals, reducing the amount of chemicals in these processes, opening new routes for more efficient processes and cleaner production in the mineral industry. Additionally, most gas dispersion parameters as bubble surface area flux (Sb), air hold up, and superficial gas velocity (Jg) will increase and probably heighten the process kinetics with decreased operating and environmental costs (energy savings, less reagents and smaller footprint).

3.4 CONCLUSIONS

A “new” technique to generate highly loaded dispersions of NBs was developed after depressurizing air that was saturated in water at low pressures (< 3 bar) and decreasing the air/water surface tension to approximately 49 mN.m^{-1}. As a result, a high density of aqueous bulk-phase NBs was created (1.6 x 10^{9} NBs.mL^{-1}), which lasted for at least two weeks. To our knowledge, this study is also the first report on the successful visualization of these aqueous

bulk-phase NBs using optical microscopy and methylene blue dye. Other results provide data on the dispersion lifetime, size and zeta potentials (as a function of pH) of the NBs and studies on the interaction between NBs and MBs. Most findings look notably important for flotation in the mineral and environmental area because NBs present a high surface area per volume and assist the capture (collision + adhesion) of particles by coarser bubbles. It is believed that this work highly contributes to the understanding of aqueous dispersion of NBs and broadens new opportunities for basic research and future applications.

3.5 ACKNOWLEDGEMENTS

The authors would like to thank all Brazilian Institutes that supported this study, namely CNPq, Fapergs, and UFRGS. We would like to especially thank Prof Adriana Pohlmann from the Chemistry Department at our University for her assistance and to all students: Luísa Heineck Neves, Luciana Tanabe, Rafaela Cazanova, Cláudio Backes and Henrique Oliveira. We are also grateful to Dr. Katia Wilberg for her constant technical cooperation.

FLOTATION OF QUARTZ PARTICLES ASSISTED BY NANOBUBBLES

Artigo publicado no periódico International Journal of Mineral Processing, volume 137, 2015, páginas 64–70.

4. FLOTATION OF QUARTZ PARTICLES ASSISTED BY NANOBUBBLES

Calgaroto, S., Azevedo, A., and Rubio, J*.

Minerals Engineering Department-PPGE3M-Universidade Federal do Rio Grande do Sul (UFRGS), Porto Alegre, Brazil; 55-51-33089479; *Corresponding author: jrubio@ufrgs.br; www.ufrgs.br/ltm

ABSTRACT

Experimental studies of flotation of quartz particles, under various conditions and cells (setups), are presented. Pure and well-characterized quartz samples were treated with a commercial alkyl ether monoamine as flotation collector with bubbles in various sizes: coarse bubbles (400–800 μm); nanobubbles (200–720 nm); and their mixtures. The nanobubbles were generated by selective separation from microbubbles, which are formed together after depressurizing-cavitation of the saturated water in air (as in pressure flotation or dissolved air flotation), at 66.1 psi saturation pressure. Flotation with single nanobubbles was not effective due to their very low lifting power or practically nil buoyancy. Yet, size-by-size flotation recoveries with coarse plus nanobubbles, compared with coarse bubbles, enhanced by 20–30 % the very fine quartz fractions (8–74 μm; Sauter diameter-d32) and slightly lowered the recoveries of coarse particles (67–118 μm; d32 diameter). Flotation of quartz samples (composites) having wide particles size distribution and results in a mechanical cell validated the overall recovery enhancement of the fines. Fine particles capture (nanobubbles enhanced the contact angle of quartz) and aggregation of the quartz ultrafines (proved with micrographs) by the nanobubbles are the main mechanisms responsible for the higher recoveries. The effect on flotation of the coarser quartz fractions, at bench scale, may be explained in terms of a reduced rising velocity of the coarse bubbles, in the presence of nanobubbles, decreasing the degree of bubbles carryover. It is expected that the use of collector-coated nanobubbles (tailor-made “bubble-collectors” and flocculants) will broaden options in fine mineral flotation. The future sustainable forms (cheaply produced) of nanobubble generation on a large scale and their injection in cells are envisaged.

Keywords: Fine flotation, nanobubbles, size-to-size quartz recoveries

4.1 INTRODUCTION

Basic and applied research involving nanobubbles, namely generation forms, basic studies, and applications is, by far, one of the fastest growing area nowadays (Agarwal, 2005; Attard, 2003; Attard et al., 2002; Hampton and Nguyen, 2010; Ohgaki et al., 2010; Ushikubo et al., 2010; Weijs and Lohse, 2013; Zimmerman et al., 2011). Today, many physical, biological, and chemical unique properties and high technological potential of the nanobubbles have been envisaged (Ahmadi et al., 2014; Calgaroto et al., 2014; Fan et al., 2012, 2010a, 2010c, 2010d; Sobhy, 2013; Sobhy and Tao, 2013; Takahashi, 2005; Zimmerman et al., 2011).

Despite the literature on nanobubbles becoming vast, nanobubble interfacial properties and their applications in many areas, including ore flotation, are interesting areas to explore (Calgaroto et al., 2014; Hampton and Nguyen, 2009; Jia et al., 2013; Najafi et al., 2007; Ohgaki et al., 2010; Takahashi, 2005; Zimmerman et al., 2011).

It is believed by a number of authors (Attard, 2003; Hampton and Nguyen, 2009; Schubert, 2005) that dissolved gases accumulate preferentially at the hydrophobic solid–water interface, and this fact has been revealed by the atomic force microscopy (AFM) (Attard, 2003; Fan et al., 2013; Hampton and Nguyen, 2010).

One of the major (and old) technical challenges in the area of mineral processing is the recovery of the fine (< 37 μm) and ultrafine (< 8-13 μm) mineral particles by flotation. Most flotation feeds are composed of a wide particle-size distribution, and flotation cells should have a wide bubble-size distribution, including fine bubbles catching the fine particles (Rodrigues and Rubio, 2007; Rubio et al., 2003; Yoon, 2000; Zhou et al., 1997). Unfortunately, this does not occur in practice and the flotation cells, available in the market, do not provide the required bubble-size distribution (Franzidis and Manlapig, 1999; Phan et al., 2003; Yoon, 2000, 1999). Thus, the earlier problem of recovering the fines and especially the ultrafines (<8-13 μm) by flotation still continues (Feng and Aldrich, 1999; Gontijo et al., 2008; Jameson et al., 2007; King, 1982; Sivamohan, 1990; Subrahmanyam and Forssberg, 1990; Szatkowski and Freyberger, 1985; Tao, 2005).

Flotation devices, namely Jet (Jameson) flotation cell and “Microcel” type column, claim that a substantial amount of bubbles < 600 μm are generated and, consequently, they should, in principle, be more suitable for fine particle recovery (Honaker and Mohanty, 1996; Jameson et al., 2007; Jameson and Manlapig, 1991; Yoon and Luttrell, 1994). The generation of fine

bubbles in a hydrodynamic cavitation tube and in columns (microbubbles injected) has been reported, claiming improvements in the flotation performance of fine fractions (Franzidis and Manlapig, 1999; Heiskanen, 2000; Honaker et al., 1996; Rubio et al., 2003; Yoon, 2000, 1999, 1993, Zhou et al., 1997, 1994).

In addition, a number of recent studies have reported some advantages in mineral flotation in the presence of nanobubbles (Ahmadi et al., 2014; Fan et al., 2013, 2010d; Fan and Tao, 2008; Sobhy, 2013; Sobhy and Tao, 2013).

The main claims are as follows: i. The nanobubbles would increase the contact angles and, subsequently, enhance the probability of flotation (coal, phosphates), mainly the bubbles-particle attachment and stability (Fan et al., 2012; Fan and Tao, 2008; Sobhy, 2013); ii. Nanobubbles would enhance particle flotation recoveries of coal particles at lower collector and frother dosages and at high kinetic flotation rate (Fan et al., 2013, 2012; Sobhy, 2013); iii. The higher flotation recoveries would be not only in the fine particles but also in the coarser coal fractions (Fan et al., 2012; Fan and Tao, 2008); iv. The presence of nano, jointly with micro- and coarse bubbles, increased the recovery of ultrafine particles of chalcopyrite with further advantages of using less collector and frother consumptions and lower power consumption.

The formation and separation (by splitting off from microbubbles) of a fraction of nanobubbles during depressurization of saturated air (66.1 psi), in water (as in DAF-dissolved air flotation) have recently been reckoned, and some physical and interfacial features were studied (Calgaroto et al., 2014). Stable (charged or not) nanobubbles are formed after the rapid depressurization of the dissolved air, and highly charged nanobubbles of a known size can be obtained either by modifying the pH or by introducing ionic surfactants (collector-coated nanobubbles). Accordingly, the sizes of the nanobubbles (200–720 nm) can be modulated by changing medium pH, and presented an isoelectric point, at about pH 4.5.

This is a continuation of the work by Calgaroto et al. (2014) on the potential application of the nanobubbles in flotation showing the results of assisted flotation of quartz at different size fractions and collector concentrations, with an injection of nanobubbles (150–350 nm), in mixtures with coarse bubbles (400–800 microns).

4.2 EXPERIMENTAL

4.2.1 Materials

Quartz powder was prepared from Brazilian quartz crystal rock by roll crushing (100 % < 1 mm) and ball milling (dry, autogenous operation), cleaning (50 % v/v HCl, rinsing with distilled/deionized water), drying (24h at 373 K), and mixing (tumbling) thoroughly. The final powder material was stored in clean plastic bags, each containing 50 g, until use for air flotation experiments (Englert et al., 2009). The quartz particles were fractioned using Mesh Tyler sieves, and the particle-size distribution of each fraction was measured using a Cilas 1064 laser particle size analyzer. Table 4.1 shows the mean Sauter diameter D32 (surface-volume) varied between 8 and 128 µm.

Table 4.1 Quartz particles size analysis in terms of mean diameter (D_{50}) and mean Sauter diameter (D_{32}).

Sieve size, mesh Tyler	**Mean Diameter (D_{50}), µm**	**Mean Diameter Sauter (D_{32}), µm**
> 65	266	128
> 100	200	110
> 200	120	65
> 400	58	34
< 400	16	8

Composite samples

Two different composite samples of quartz particles were prepared by blending all the previously separated fractions. Composite sample 1 had equivalent amounts of all fractions (20 % of each fraction), and composite sample 2 was made up using different amounts of each fraction, as shown in Table 4.2.

Table 4.2. Flotation of quartz particles. Preparation of composite samples

Siever size, mesh Tyler	**Siever size, µm**	**Composite Sample 1 Mass percentage, %**	**Composite Sample 2 Mass percentage, %**
> 65	> 212	20	40
> 100	< 212	20	40
> 200	< 150	20	10
> 400	< 75	20	5
< 400	< 37	20	5

Chemicals

Flotigam EDA 3B (Clariant®), a commercial flotation quartz collector that corresponds to an alkyl ether monoamine, with chemical formula $R–O–(CH_2)_3–NH_2$, partially neutralized with acetic acid (Clariant®, Technical Bulletin, Div. Functional Chemicals/Mining). NaOH and HCl, from Vetec®, were used for pH adjustments (kept between pH 6.8 and 7.2). Deionized water was used throughout the flotation work.

4.2.2 Methods

Generation of Coarse Bubbles

Here, coarse bubbles corresponded to bubbles generated by passing air through a fritted glass plate. The diameter of bubbles (measured photographically) varied between 0.4 and 0.8 mm with an air flow rate of 0.1 $L.min^{-1}$ in the presence of 10^{-4} M Flotigam EDA 3B.

Generation of Nanobubbles

The bubbles were generated by depressurizing air-saturated water solutions at a high flow velocity through a steel needle valve (2-mm internal diameter: Globo 012 - Santi®) into an empty glass column (50 cm high; 2 cm inner diameter). The saturation of air in water was achieved in a steel vessel containing an internal glass container with a height of 15 cm, an inner diameter of 12 cm, and a wall thickness of 1 cm. The container had a height of 14 cm, an inner diameter of 10 cm, a wall thickness of 0.5 cm, and a real capacity of 0.7 L (Calgaroto et al., 2014).

The depressurization followed by cavitation occurred, and both micro- and nanobubbles are generated. Thus, a procedure was carried out by simply leaving the microbubbles levitate and abandoning the glass column, during 3 min (Figure 4.1). Then, getting profit that nanobubbles are very stable, a sampling volume of 150 mL was bypassed from the column feeding the Zeta Sizer Nano ZS (red badge) - ZEN3600 – Malvern® Instrument to measure their average size.

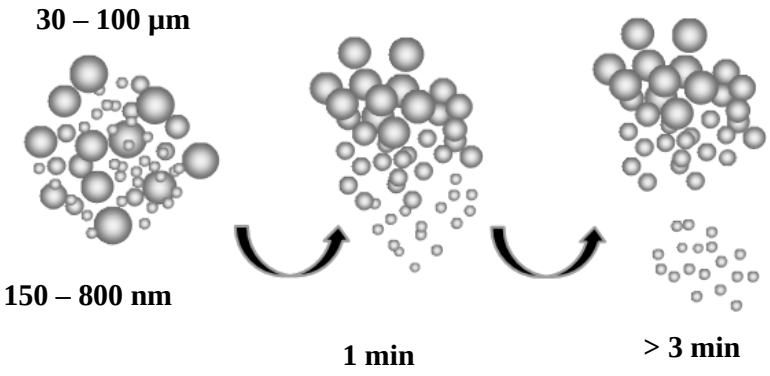

Figure 4.1. Separation by uprising of the microbubbles, from mixtures with nanobubbles.

Flotation

The flotation of quartz was conducted with classified-sized fractions and with the composite samples, prepared by blending all the quartz fractions studied as described in Table 4.2.

Thus, flotation tests were carried out with different setups:

i. Flotation with coarse bubbles in a Hallimond Tube;

ii. Flotation in a Hallimond Tube with coarse and nanobubbles;

iii. Flotation in a Denver type cell with and without injection of nanobubbles.

System 1 - Flotation with coarse bubbles. The flotation tests were performed in a 0.2-L capacity typically modified Hallimond Tube with 270-mm height and 18-mm inner diameter (Figure 4.2). This flotation setup had an intermediate small column to avoid (diminish) some particle entrainment. The air used in the process was generated by a compressor connected to a flow meter controlling the flow rate of the air (0.2 $L.min^{-1}$) passed through a fritted porous glass. The collector concentration varied between 0.3 and 1 $mg.g^{-1}$ (i.e. collector/quartz mass ratio), and the weight ratio of quartz used was 2% (by weight) in all flotation tests (1 min conditioning time and 2 min flotation). The flotation of quartz was carried out for 2 min at different collector/quartz mass ratios and 2 % solids by weight.

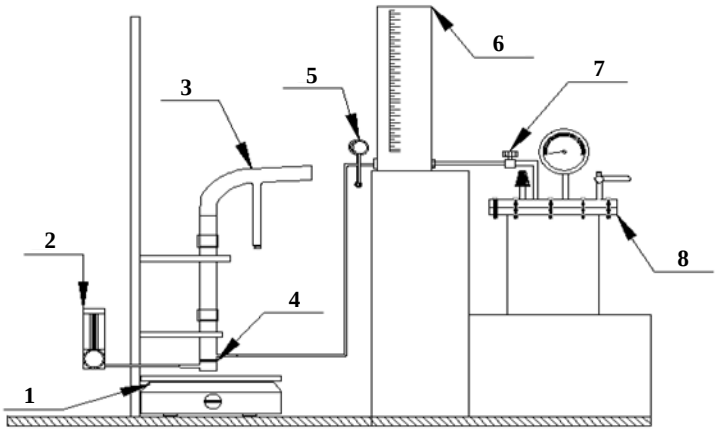

Figure 4.2. Experimental setup (Hallimond Tube + Nanobubble injection system) for the generation of bubbles and flotation tests with coarse and with nano and coarse bubbles: Flotation with coarse bubbles does not use the nanobubbles injection system. (1) magnetic stirrer; (2) flow meter; (3) Hallimond Tube; (4) porous plate; (5) clamp; (6) micro column; (7) needle valve; (8) saturator vessel.

System 2 – (Coarse bubbles + NB). The procedure (Figure 4.2) employed the same modified Hallimond tube (200 mL capacity) endowed with two air inlets at the base: one receiving the air flow (coarse bubbles) and another connected to a microcolumn (500 mL capacity), to inject the nanobubbles. The nanobubbles were generated and separated from the microcolumn following the procedure described in Figure 4.1, and were injected at a recycle ratio of 20% by volume. All other conditions were similar to System 1.

System 3 – Flotation of quartz in a mechanical cell. The bench-scale flotation experiments were performed using a 2 L mechanical Denver type flotation cell by conditioning 200 g fine quartz particles (< 90 μm) with 1 mg amine/g quartz.

In the tests conducted with nanobubbles, a nanobubble bearing aqueous dispersion was previously prepared by depressurization (P_{sat} = 5 bar) and used during conditioning of the quartz with amine. The dispersion was stirred (750 rpm) for 2 min while adjusting the pH (6.9). Then, flotation was performed during 4 min with impeller speed and air flow fixed at 750 rpm and 6 L/min, respectively.

All flotation tests were executed in duplicates at room temperature (297±1 K) at pH 6.2±0.5 of the (Flotigam EDA 3B) solution (6.2±0.5). The floated was filtered through a 14-μm mean pore size filter paper, dried in a laboratory furnace at 373 K, and weighed at room temperature. Recoveries corresponded to the results obtained by the ratio mass of floated particles/total mass

of particle feed. Some of the products were analyzed by their particle size in a Cilas 1064 analyzer.

Contact angle measurements

Quartz (rock crystal) mineral particles were chosen due to their high purity and because they were easily obtained. These particles were carefully manually broken in an agate mortar, and two particles (approximately 0.5-cm long) were selected for the studies.

Figure 4.3 shows the details of the experimental rig. A low amine concentration solution (10^{-6} M) at pH 6.9 was used to make the quartz hydrophobic and also employed in the nanobubble generation. A steel saturation vessel to dissolve the air in water was equipped with an internal container made of glass (40 cm high, 10 cm in diameter, and 0.5 cm thick; 0.7 L effective capacity). The depressurization-cavitation stage employed had a 2-mm internal diameter needle valve (Globo 012-Santi®, steel made).

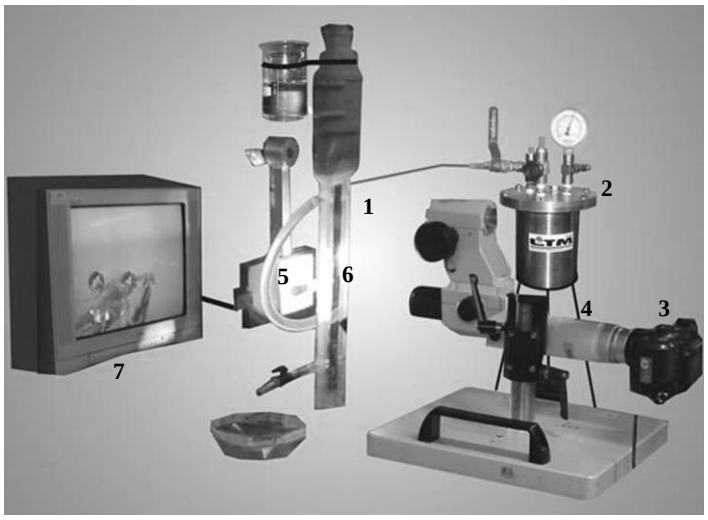

Figure 4.3. Experimental set-up for contact angles measurements at the quartz/ microbubbles interface, with and without nanobubbles: (1) flat cell; (2) saturator vessel; (3) digital camera; (4) stereomicroscope; (5) white light source; (6) quartz particle; (7) monitor for image reproduction.

The experimental setup consisted of a system injecting the saturated water with air through a needle valve into a flat acrylic cell and a stereomicroscope (Zeiss Stemi SV11) coupled to a digital camera (Sony NEX-3). The cross-section of the flat cell was rectangular and 1.5 cm deep, 28 cm high, and 4 cm long. The center of this cell included an orifice attached to a glass tubing (0.1 cm in diameter and 7.5 cm long) containing a quartz particle adhered at the end. The flat cell also contained two orifices designed for the inlet and outlet entrance of aqueous

solutions allowing the liquid phase to flow through to the particle. The quartz particles and materials were carefully cleaned before all studies using a solution of hydrochloric acid (10% HCl), followed by immersion in a sulfochromic solution for 0.5 h and rinsing thoroughly with deionized water.

Quartz particle aggregation with nanobubbles

Optical microphotographs of hydrophobic (with 1mg amine/g quartz) fine quartz aqueous dispersion, in the presence and absence of nanobubbles, were taken. An optical microscope Olympus, model BX41 was employed having an objective magnification of 40x and 100x coupled to a Microscope Digital Camera of high-performance, Olympus DP73 (17.28 megapixel of resolution).

Rising velocity of bubbles

The rising velocity of bubbles generated in the Hallimond tube fritted glass was measured by monitoring the time taken by a cloud of bubbles to surpass a certain distance (10 cm) in a lab column (2 cm diameter). Results were the average of at least 4 measurements evaluating the effect of amine on the rising velocity of coarse mixtures with nanobubbles.

4.3 RESULTS

The first finding is that no flotation was attained with the nanobubbles alone. This was already expected because of the extremely low lifting power of the minute bubbles and insignificant buoyancy in water (Calgaroto, et. al, 2014).

Figure 4.4 shows size-by-size flotation recoveries of quartz particles by coarse bubbles (400–800 microns) and nanobubbles (200-800 nm). The results revealed that nanobubbles improved the recovery of fine fractions and slightly decreased the capture of coarse particles.

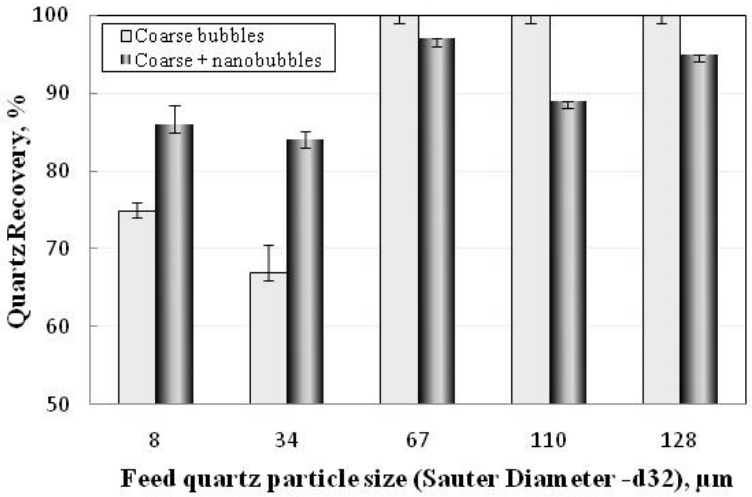

Figure 4.4. Flotation quartz recoveries as a function of their mean Sauter diameters with and without nanobubbles. Conditions: pH 6.9 and 1 mg amine collector concentration/g quartz.

Figure 4.5 shows the comparative results of flotation of the < 37 micron fractions, and Figure 4.6 shows the results with the coarser fraction (> 212 microns), as a function of collector concentration. Again, results demonstrated the higher flotation efficiency for the fines and the lower flotation efficiency for the coarse particles in the presence of the nanobubbles.

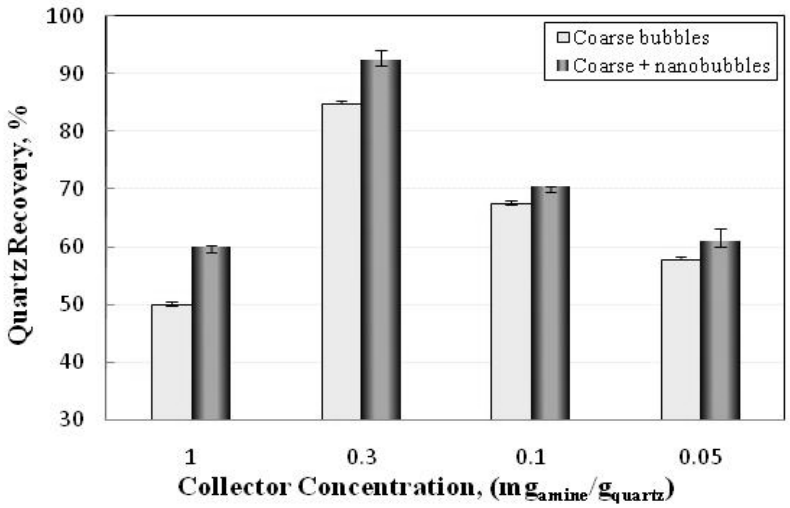

Figure 4.5. Flotation quartz recoveries for the < 37 microns fraction (fines) as a function of amine collector concentration, with and without nanobubbles at pH 6.9.

Tables 4.3 and 4.4 summarize the comparative results of flotation of quartz in composites 1 ("fine"-(D32) = 32 µm) and 2 (¨coarse"-(D32) = 57 µm) samples. Results validated size-to-size flotation results and showed, in the composite 1, much higher separation efficiency for the fines (< 74 µm) and ultrafines (<8 µm). Recoveries were higher in about 20 % with low standard deviation and fine particles size in concentrates. With composite, much coarser feed, higher

quartz recoveries were obtained with the coarse bubbles, with not much effect of the nanobubbles.

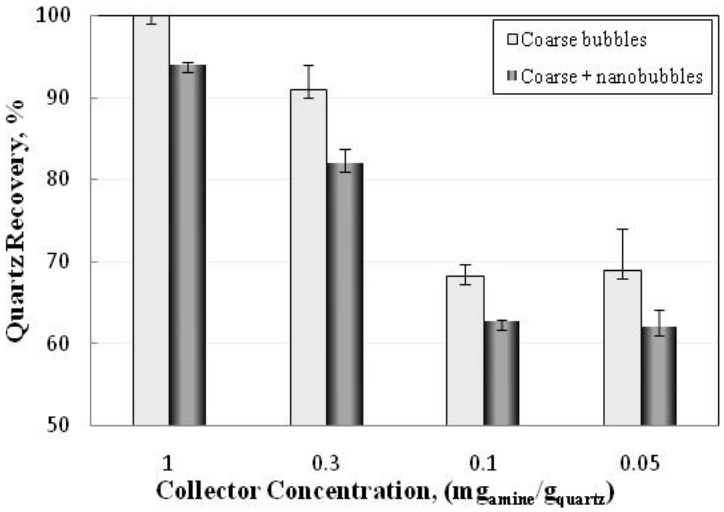

Figure 4.6. Flotation quartz recoveries for the >212 microns fraction (coarse) as a function of amine collector concentration, with and without nanobubbles at pH 6.9.

Table 4.3. Flotation of quartz particles (composite sample 1) with coarse and with a mixture of coarse and nanobubbles. Conditions: Mean Sauter diameter of feed (D32) = 32 µm; 2 % of solids; amine concentration = 0.3 $mg.g^{-1}$ quartz; pH 6.8. Averaged values of triplicate tests.

System used	Mean diameter (D32) of flotation concentrate, µm	Recovery, %	Standard deviation, %
Coarse bubbles	44	44	4.5
Coarse bubble + Nanobubbles	33	64	2.3

Table 4.4. Flotation of quartz particles (composite sample 2). Conditions: Mean Sauter diameter of feed (D32) = 57 µm; 2 % of solids; amine concentration = 0.1 $mg.g^{-1}$ quartz; pH 6.8. Averaged values of triplicate tests.

System used	Mean diameter (D_{32}) of flotation concentrate, µm	Recovery, %	Standard deviation, %
Coarse bubbles	31	61	2.7
Coarse bubble + Nanobubbles	35	65	1.8

Table 4.5 shows that the flotation, in the mechanical cell, was more rapid in the presence of nanobubbles and that at 9 min the full recovery was about 3 % higher. These results validate results in the Hallimond tube and prove the benefits of using nanobubbles.

Table 4.5. Flotation of quartz particles in a mechanical cell with and without nanobubbles. Conditions: pH = 6.9; conditioning time = 2 min; 20 % solids; impeller speed = 750 rpm; air flow = 6 L/min.

	Recovery (%), 2 min	**Recovery (%), 4 min**	**Standard deviation (%)**
Without Nanobubbles	24	81	0.24
	26	81	
With Nanobubbles	39	83	0.29
	37	85	

4.4 DISCUSSION

The results obtained may be explained by various mechanisms that appear to be operating simultaneously. Most important is the role in enhancing quartz contact angle and aggregation of the fines/ultrafines.

Thus, quartz recoveries, assisted with nanobubbles, appear to be a result of the following phenomena:

1. Adsorption of amine molecules onto quartz particles, with the polar head toward the surface (electrostatic interaction), turning particles hydrophobic;

2. Adsorption of amine molecules onto the nanobubbles by the hydrophobic tails surrounding the bubbles (hydrophobic interaction). Here, bubbles become charged, depending on pH and adsorption density (Calgaroto et al., 2014);

3. Adhesion of the coated bubbles with amines onto the coarser bubbles: The nanobubbles may adhere (Fan et al., 2012) alone or coated with amine (collector-loaded bubbles);

4. The contact angle at the quartz/bubble interface increased as a result of adhesion of the collector-coated quartz particles with nanobubbles;

5. Adhesion of nanobubbles (coated or not with amine molecules) onto coarser bubbles;

6. The nanobubbles, jointly with amine, reduce the coarse bubble size and decrease the rising velocity of these bubbles;

7. Aggregation of hydrophobic quartz particles and flotation of the aggregates by the consortium nanobubble-coarse bubbles.

Figure 4.7 shows contact angle values at the air/hydrophobic quartz interface without (a) and with nanobubbles (b). As expected, the nanobubble (not visible in this microphotography) enhanced the contact angle of the amine-coated quartz, showing its collector characteristic.

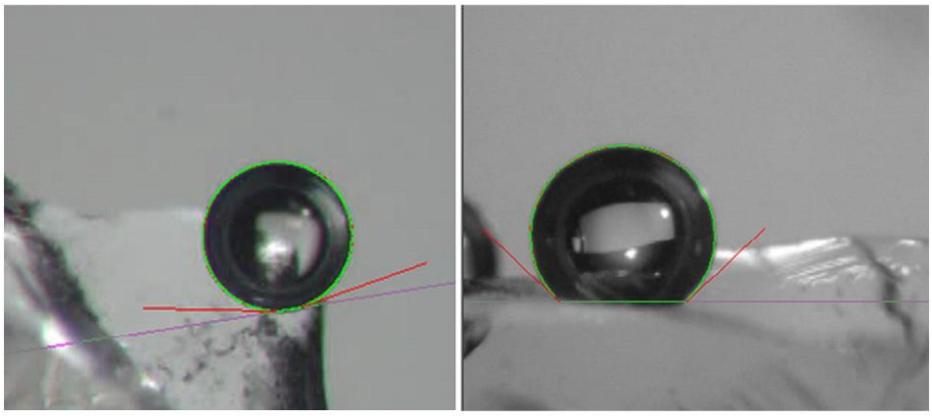

(a) (b)

Figure 4.7. (a) Mean contact angle: 18°, standard deviation = 3.6° at a quartz/water interface: photomicrograph of a microbubble adhered to quartz, in 10−6 M, without nanobubbles; (b) Mean contact angle: 46°, standard deviation= 7° at a quartz/water interface: photomicrograph of a microbubble adhered to quartz, in 10−6 M, with nanobubbles.

Figure 4.8 illustrates the aggregation of amine-coated quartz fines in the presence of nanobubbles, showing the high amenability of nanobubbles for hydrophobic moieties. It is believed that this finding is highly important for flotation of fine/ultrafine particles, because it increased the particle size, enhanced particle capture by bubbles, and revealed that nanobubbles behave not only as a secondary collector but also as an aggregating reagent.

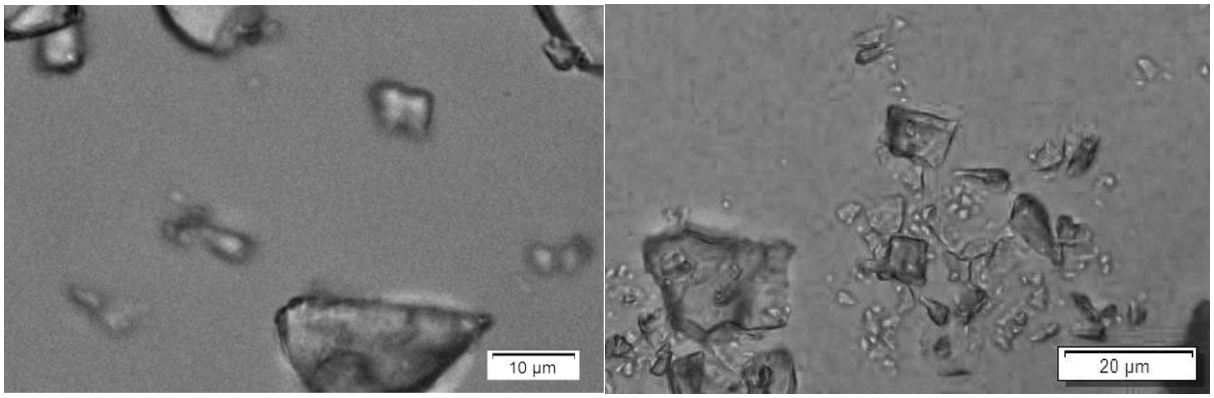

(a) (b)

Figure 4.8. Microscope images of fine quartz particles suspensions (100 mg.L^{-1}) in a low concentration amine solution (10^{-6} M). (a) Without nanobubbles; (b) With nanobubbles (showing aggregation of fine quartz particles).

Table 4.6 show results of rising velocity of bubbles in the presence of amine with and without nanobubbles. The effect of surfactants on reducing bubble size is known (Laskowski, 1989) but the presence of nanobubbles further reducing this velocity should be explained by some retarding, pull-back phenomenon of the nano-coarse bubble assembly.

Table 4.6. Rising velocities of bubbles as a function of amine concentration, with and without nanobubbles.

	Rising velocity of bubbles, ($cm.s^{-1}$)		
	Without amine	Amine, 10^{-5} M	Amine, 5.10^{-5} M
Coarse bubbles	4.8	4.6	2.6
Coarse bubbles + Nanobubbles	3.9	3.7	1.4

Regarding the entrainment of quartz by rising bubbles (hydrodynamic carryover), this should follow the lifting capacity of the nano-coarse bubble units. Fan et al. (2012) found that the up-rising velocity of the coarser bubbles decreases in the presence of nanobubbles, but no explanation or numbers, were not given. This phenomenon might lead to different effects as to whether flotation is either batch or continuous. On the one hand, if the bubble rise slows down, the particle hydraulic entrainment will decrease, reducing quartz particle recoveries. However, the residence time is enhanced and this situation might improve coarse particle capture by bubbles in the continuous flotation. This would explain our results with the mechanical cell and those obtained by Fan and Tao (2008) and Fan et al. (2013), where the nanobubbles jointly with microbubbles enhanced the flotation of phosphate in all size fractions.

4.5 CONCLUSIONS

The injection of small bubbles appears to be an interesting alternative, and many scientific articles have proved that fine particle capture (magnitude and kinetic) is enhanced in the presence of microbubbles, nanobubbles, or both. Here, similar to recent articles, the injection of nanobubbles (200–720 nm) along with conventional coarse bubbles (400-800 µm) improved the flotation recoveries of quartz fines and ultrafines. Size-by-size flotation with coarse plus

nanobubbles, compared with coarse bubbles, improved the recoveries of the very fine quartz by 20–30 % and slightly lowered the recoveries of coarse particles in small Hallimond bench-scale tests. Results are explained by the enhancement of fine/ultrafine (< 8 -74 μm) particle capture and by the slower rising velocity and entrainment by the coarse bubbles, in the presence of nanobubbles. Higher contact angles and quartz fine aggregation in the presence of nanobubbles appears to be the most important mechanisms involved. It is believed that the future challenge is to generate and inject nanobubbles economically, on a large scale, using high throughput and for long periods. Research must continue at batch and pilot scale in conventional cells.

4.6 ACKNOWLEDGMENTS

The authors would like to thank all the Brazilian Institutes supporting this research, namely CNPq, Fapergs, and UFRGS. Special thanks are due to undergraduate students Luísa Heineck Neves and Marcio Nicknig and to all students at the laboratory. The authors are also grateful for the friendly atmosphere.

SEPARATION OF AMINE-INSOLUBLE SPECIES BY FLOTATION WITH NANO AND MICROBUBBLES

Artigo publicado no periódico Minerals Engineering, volume 89, 2016, páginas 24–29

5. SEPARATION OF AMINE-INSOLUBLE SPECIES BY FLOTATION WITH NANO AND MICROBUBBLES

Calgaroto[1], S., Azevedo[2], A., Rubio[2,3], J.

[1]Instituto de Química; [2]Departamento de Engenharia de Minas-DEMIN, Universidade Federal do Rio Grande do Sul, Av. Bento Gonçalves, 9500, Campus do Vale, Prédio 43819 - Setor 6, 91501-970, Porto Alegre-RS, Brazil; www.ufrgs.br/ltm [3]Corresponding author: jrubio@ufrgs.br

ABSTRACT

Amines (alkylamines-ether amines) are employed on a large scale to separate iron ores by reverse flotation of the gangue particles (mostly quartz and silicates). Quartz gangue particles

coated with amine collector are dumped in tailings dams as concentrated pulps. Then, the fraction of the amines that detach from the surfaces and the portion that is soluble in water, contaminate surface and ground-water supplies. This work presents a novel flotation technique to remove decyl-trimethyl-ether-amine (collector employed in Brazilian iron mines) from water. This amine forms precipitates at pH>10.5 which are removed by flotation with microbubbles (MBs: 30-100 µm) and nanobubbles (NBs: 150-800 nm). Bubbles were generated simultaneously by depressurization of air-saturated water (P_{sat} of 66.1 psi during 25 min) forced through a flow constrictor (needle valve). The flotation by these bubbles is known as DAF-dissolved air flotation, one of the most efficient separation technologies in water and wastewater treatment. Herein, best results (80% amine removal) were obtained only after selective separation of the MBs from the NBs exploring the fact that while the NBs remain dispersed in water, the MBs rise leaving the system. The MBs, because of their buoyancy, rise too rapidly and do not collide and adhere appropriately at the amine colloids/water interface, even causing some precipitates breakage. It was found that the "isolated" NBs attach onto the amine precipitates; aggregate (flocculate) them and entrain inside the flocs before rising by flotation. Because of the low residual amine concentration in water (6 $mg.L^{-1}$), it is believed that this flotation technique have potential in this particular treatment of residual amine-bearing effluents.

Key words: Amines, flotation, nanobubbles, microbubbles, environmental

5.1 INTRODUCTION

Amines are organic compounds widely used in the industry. The consumption of these reagents as flotation agents (collectors) in iron and potassium mining is growing fast in Brazil (Araujo et al., 2010). In the reverse flotation of iron ore the process consists of a selective separation of quartz/silicates particles (gangue material) from the valuable iron oxides. Thus, the amine collector is adsorbed onto quartz particles surfaces and is removed from the system as a mineralized froth and dumped in tailings dams.

It is estimated that approximately 5500 tons of amine derivatives per year are used in flotation processes only in Brazil, values that will continue to increase in the next few years, due to the more complex (disseminated-locked particles) and low feed grade of values in future ores (Araujo et al., 2010).

The use of amines in mining industry has been a matter of concern because of various environmental problems involved; amines are accumulated in large quantities in tailings dams and present incomplete degradation (Araujo et al., 2010; Baltar et al., 2002; Chaves, 2001). Another problem (at least in Brazil) associated with wastewaters containing amines is the nonexistence of specific protective legislation (Neder and Leal Filho, 2005; Peres et al., 2000).

High levels of fatty amines can be harmful and cannot be directly disposed into aquatic bodies (Newsome et al., 1991; Schultz et al., 1991). More, their toxicity, degradation and byproducts formed are issues which are not completely understood. Studies on amine biodegradation have been reported by Araujo et al., (2010) and Chaves (2001).

Chaves (2001) studied the toxicity of an ether amine (2% by weight concentration - Akzo Nobel®) on *Tenebrio molitor* larvae and found that about 50% of the insect population expired in 7 days. The same author evaluated the effect of acute toxicity of these amines to albino Wistar rats, concluding that the absorption of the ether amine orally by the body is low, but the toxicological effects when it is absorbed by the body (intraperitoneal absorption) caused leukopenia, leading to death of 50% of the population. Also, it was concluded that the degradation time of these ether amines in tailings dams would be approximately 12 days. But, the byproducts species are not known and the emission, in large quantities of nitrogen compounds still continues.

DAF-dissolved air flotation is a well-known separation technology for removing colloids, precipitates, flocs, oily drops, fine pollutants and ultra-fines solids (Edzwald, 2010, 1995; Karhu et al., 2014; Y. Liu et al., 2012; Oliveira and Rubio, 2009; Rodrigues and Rubio, 2007; Rubio et al., 2002).

The amines are precipitated in alkaline medium, after a decrease of their solubility at pH > 10.5 (Fuerstenau et al., 1985; Laskowski, 2013, 1989; Smith and Akhtar, 1976). Herein, the amine was precipitated at pH 10.8 and the precipitates or flocs removed by flotation.

This work is a continuation of a series on flotation of pollutants which also explores the properties of nanobubbles (NBs) on flotation systems (Calgaroto et al., 2014, 2015). Recently, our research group discovered and measured the simultaneous generation of microbubbles (MBs) and NBs in DAF, after depressurization of a flux of water containing dissolved air in a flow constrictor (Calgaroto et al., 2014, 2015). The separation of the NBs from the MBs and their flotation properties by deferential rising velocities, in water, was another finding (Calgaroto, 2015).

5.2 EXPERIMENTAL

5.2.1 Materials and reagents

Solutions (2 to 500 $mg.L^{-1}$) of a commercial amine: Flotigam EDA 3B (Clariant®), were prepared using deionized water (reverse osmosis) and used throughout the work. This reagent is a cationic decyl-trimethyl-ether-amine with molecular weight of 195 $g.mol^{-1}$ (molecular formula: $[R\text{-}O\text{-}CH_2)_3\text{-}NH_3]^+ CH_3COO^-$, where R is a hydrocarbon chain of approximately ten carbon atoms; molecular weight).

Solutions of pre-polymerized coagulant Acquafloc 18 ($Al_n(OH)_mCl_{3n-m}$; cationic; Faxon®) and NaCl (supplied by Synth®) were employed for flocculating the amine precipitates.

A buffer solution, composed of bromocresol green, potassium biphtalate and 0.1 M NaOH was used in the colorimetric method for determination of the residual content of amine. Chloroform (Merck®) was used as solvent in the chemical extraction of amine and NaOH and HCl solutions were employed for pH adjustments.

5.2.2 Methods

Characterization of the amine precipitates

The residual turbidity (NTU) of solutions was measured with a nephelometer (Hach® 2100N) in order to follow the precipitation of the amine Flotigam EDA 3B at pH 10.8. Measurements (triplicated runs) were performed at different amine concentrations and pH 10.8 (standard deviations were < 1 %). The higher the turbidity, the greater the concentration of the colloidal precipitates.

The amine precipitates were characterized by their size and zeta potential. The particle size distribution and the zeta potential of the nano sized amine precipitates were determined using a Zeta Sizer Nano ZS (red badge) - ZEN3600 – Malvern® Instrument. The particle size distribution of the micrometric precipitates was determined by laser diffraction (Cilas® 1064).

The ZetaSizer Nano employs a Laser Doppler Micro-electrophoresis technique whereby an electric field is applied to the precipitates migrating at a velocity that is dependent on zeta potential. This velocity is measured by laser interferometry-M3-PALS (phase analysis light scattering), which enables the calculation of the electrophoretic mobilities, then converted to zeta potential (millivolts) using Smoluchowski's equation (Hunter, 1981). This equipment uses

dynamic light scattering (DLS) for size measurements (Berne and Pecora, 2000). Measurements of zeta potential and size were performed at a scattering angle of 90°, a wavelength of 290 nm and a temperature of 296 K. Each zeta potential and size determination corresponded to mean values calculated from 90 measurements (forty-five for two different samples).

The experiments were performed in duplicate with three runs of analysis for each sample and the mean values were calculated with associated errors corresponding to the standard deviation of the data.

Jar Test for flocculation of amine precipitates

These studies were carried out in Jar Test® equipment (0.6 L of jars capacity). The solutions of Flotigam EDA 3B, at various concentrations (2 - 500 $mg.L^{-1}$; pH = 11) were destabilized with an inorganic salt (5 $mg.L^{-1}$ NaCl) and flocculant (5 $mg.L^{-1}$ Acquafloc 18).

The resulting suspension was submitted to a rapid stirring (120 rpm) for 1 min to promote the diffusion and adsorption of destabilizing reagents. This was followed by slow stirring (50 rpm) for 1 min to build up the flocs of the amine precipitates. This was necessary to strengthen the precipitates and improve their flotation.

Flotation studies

Removal of precipitates (flocs) of amine by DAF (flotation with MBs +NBs)

Here, DAF will refer to conventional flotation with MBs and NBs and F-NBs will refer to flotation with only NBs, after separation of the MBs. MBs have been measured in our laboratory as having Sauter diameters varying between 30 and 100 μm (Rodrigues and Rubio, 2003) and NBs between 300 and 800 nm, measured in the same ZetaSizer Nano ZS (Calgaroto et. al, 2014).

Flotation studies were carried out using the same setup shown as in Calgaroto et al., (2015). The bubbles were generated by depressurizing air-saturated water solutions (flow rate of 0.2 $L.min^{-1}$) forced through a steel needle valve (2-mm internal diameter: Globo 012 - Santi®).

The saturation of pure deionized water in air was achieved in a stainless steel vessel with a height of 15 cm, an inner diameter of 12 cm and a wall thickness of 1 cm. The vessel enclosed an internal glass container of with a height of 14 cm, an inner diameter of 10 cm, a wall thickness of 0.5 cm and a capacity of 0.7 L. The air was dissolved, in batch runs, at 66.1 psi pressure for 25 min. Inline air filters were employed to purify the depressurized air in water.

The flotation of the precipitate flocs followed, using 150 mL of water with bubbles in a micro column (240 mL capacity; h= 280 mm; diameter = 23 mm) containing an air inlet at the base.

Removal of precipitates (flocs) of amine by flotation with NBs (F-NBs)

Figure 5.1 shows the flotation set up, which is similar to that used in 2.2.3.1, but includes a glass column (2 L capacity; h = 250 mm; diameter = 100 mm) employed to separate the NBs from the MBs. This column had two air inlets at the base: one entry receiving the depressurized flow (NBs and MBs) and another connected to the flotation column to inject the isolated NBs.

The separation of the bubbles proceeded simply letting the MBs rise (about 4 $cm.min^{-1}$), for 3 min, abandoning the glass column, leaving the NBs dispersed in the water (Calgaroto et. al., 2015). A fixed volume of NBs was injected (recycle ratio of 20% by volume) in the flotation cell through a latex tube.

Figure 5.1. Experimental setup for the generation of bubbles, separation of the MBs and NBs and flotation with NBs: (1) magnetic stirrer; (2) flotation cell (3) clamp (NBs outlet); (4) MBs-NBs separation column; (5) needle valve; (6) saturator vessel.

In both studies (DAF and F-NBs), the flotation lasted 2 min and the results corresponded to the measurements performed in triplicate runs. The samples were collected from the bottom of the column and analyzed by the content of amines using an analytical colorimetric technique. Results are expressed as amine removal (%) and residual amine ($mg.L^{-1}$) in the treated solutions and the experimental error is associated with the standard deviation of the triplicate runs.

<u>Determination and quantification of amine</u>

The residual concentration of the Flotigam EDA 3B was determined using a colorimetric method, by placing in a separating funnel 25 mL of chloroform, 10 mL bromocresol green

buffer solution and 10 mL of sample (Araujo et al., 2009). After agitation, the liquid became yellow, indicating the presence of amine. After decanting the chloroform fraction, its absorbance was measured using the spectrophotometer (Merck® model SQ 118; λ = 405 nm). A blank reference was made with the chloroform alone.

Standard solutions of 5, 10, 15 and 25 $mg.L^{-1}$ of amine (Flotigam EDA 3B) were used to construct the analytical calibration curve (Figure 5.2).

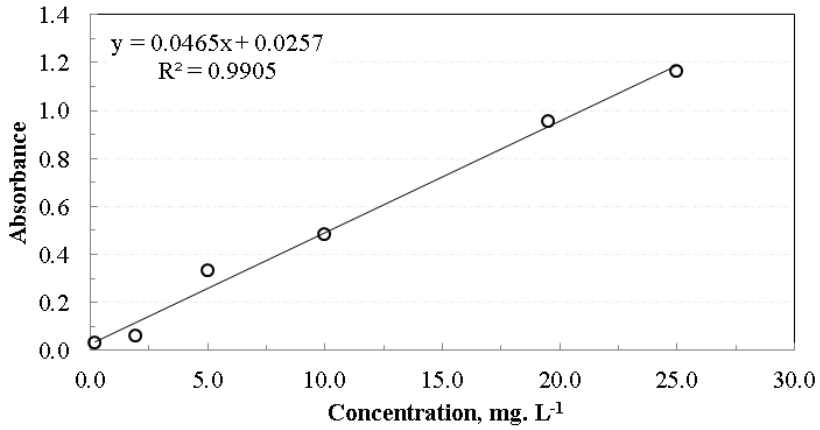

Figure 5.2. Calibration curve for amine (Flotigam EDA 3B) concentration. Absorbance values of the bromocresol green-amine complex.

Photomicrographs of amine precipitates and NBs

Optical microphotographs of amine precipitates in aqueous dispersion were taken in the presence and absence of NBs. An optical microscope Olympus® model BX41 was employed with an objective magnification of 400x and 1000x coupled to a Microscope Digital Camera of high-performance, Olympus DP73 (17.28 megapixel of resolution). In this procedure, the amine precipitates were conditioned with NBs aqueous dispersion, produced and separated from MBs as described before (section 2.2.3.2), in a ratio of 1:1 (volumetric ratio) for a period of 5 min at slow mixing (50 rpm). After that, 2 drops of sample was put between the microscope glass slide and the cover slip for image acquisition. Blank test was performed using the same volume of deionized water (without NBs).

5.3 RESULTS AND DISCUSSION

5.3.1 Formation of amine precipitates species

Smith and Akhtar (1976) were the first to discover that amines are insoluble in alkaline medium (pH > 10). They constructed a species diagram, as a function of pH, which has been extensively cited (Fuerstenau et al., 1985; Laskowski, 1989).

Validation of these data was performed here by monitoring turbidity measurements as a function of concentration of the ether amine, at pH 10.8 (Figure 5.3). The increase in turbidity is an indication of the colloidal precipitates formation. Above 150 $mg.L^{-1}$, the turbidity of the amine solutions rapidly increased before formation of bulky precipitates.

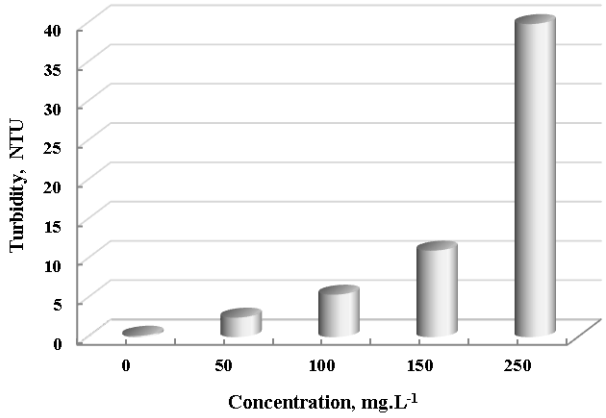

Figure 5.3. Aqueous solution turbidity values as a function of decyl-trimethyl-ether amine (Flotigam EDA 3B-Clariant ®) concentration, at pH 10.8.

These insoluble species of amines have a wide particle-size distribution, from visible precipitates (mm), colloidal precipitates (microns) and invisible nanoparticles (nanometers). Figure 5.4 shows the particle size distribution of the amine precipitates formed at pH 10.5 and amine concentration of 250 $mg.L^{-1}$, determined by laser diffraction (Cilas® 1064). After 5 min, most of the precipitates corresponded to colloidal units sizing about 130 µm, which can be readily seen (milk like); then a small fraction of a few microns (<10 µm); and the rest are the nano sized precipitates (< 1 µm), measured in the Nano ZetaSizer (Figure 4).

Figure 5.5 shows that the nanoparticles present an isoelectric point at about pH 11, which coincides with the precipitation pH and with a maximum size at almost 600 nm. When particles

are fairly charged, the particles are smaller than 200 nm suggesting that repulsion forces may prevents their growth.

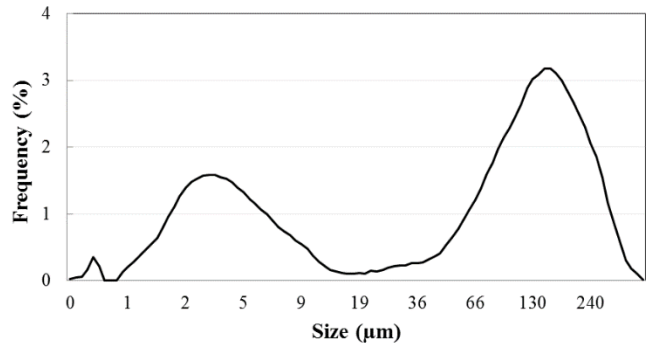

Figure 5.4. Particles size distribution of the amine precipitates at pH 10.5, after 5 min. 250 mg.L^{-1} decyl-trimethyl-ether amine (Flotigam EDA 3B-Clariant ®).

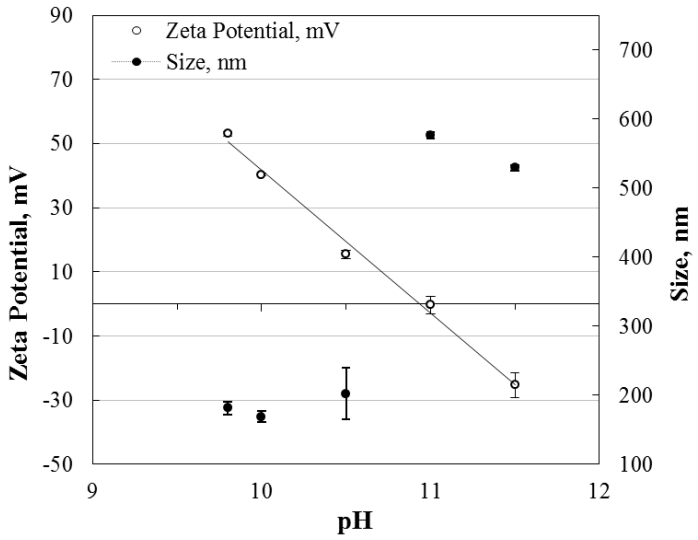

Figure 5.5. Size and zeta potential of the amine nano-precipitates (250 mg.L^{-1} decyl-trimethyl-ether amine - Flotigam EDA 3B) as a function of pH. The measurements were done 30 min after pH adjustment to guarantee the total formation of amine nano – precipitates. The zeta potential data are adjusted with linear tendency line.

5.3.2 Removal of amine precipitates by flotation

Figure 6 shows comparative amine removal by DAF and by F-NBs and Table 1 summarizes results with and without the polyaluminum flocculant. The results clearly showed that the removal of the amine precipitates was more efficient by F-NB and that the polyaluminum increased this efficiency, probably because aggregates/flocs are stronger and more amenable to flotation (Solari and Rubio, 1984).

It is believed that, in the presence of MBs, which present faster rising velocities, the contact time (microbubble/precipitates) is rather short for bubble attachment. Also, some precipitate breakage was observed visually.

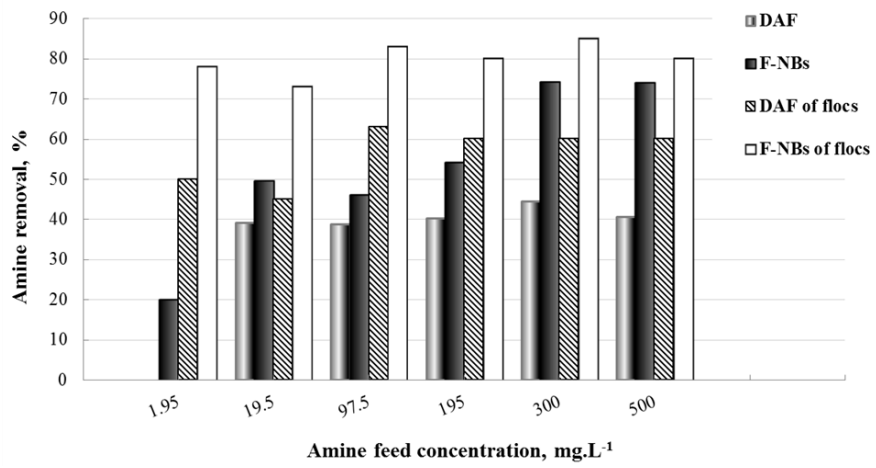

Figure 5.6. Comparative removal of precipitated decyl-trimethyl-ether amine (Flotigam EDA 3B-Clariant ®) by DAF and F-NBs (Flotation with NBs only) and with polyaluminum flocculant (DAF of flocs and F-NBs of flocs), after precipitation at pH 10.8.

Table 5.1. Comparative amine removal efficiencies between DAF and F-NBs. Effect of feed amine concentration and polyaluminum chloride coagulant (5 mg.L^{-1} Acquafloc 18)*.

Feed amine concentration, mg.L^{-1}	Residual amine concentration after DAF, mg.L^{-1}	Residual amine concentration after F-NBs, mg.L^{-1}	Residual amine concentration after flocculation + DAF, mg.L^{-1}	Residual amine concentration after flocculation + F-NBs, mg.L^{-1}
0.195	0.1	0.08	0.1	0.02
1.95	0.8	0.6	0.8	0.02
19.5	9	7	10	6
195	78	56	57	35
500	322	140	250	160

* = This concentration was chosen as the most suitable for flotation in terms of size and weight of the flocs formed.

Conversely, the NBs are known to interact with hydrophobic surfaces and a number of authors (Hampton and Nguyen, 2009; Attard, 2003; Schubert, 2005) have observed that the NBs (so-called interfacial NBs) accumulate as clusters or pancakes at the hydrophobic solid–water interface. This fact has been revealed by atomic force microscopy (AFM) (Attard, 2003; Fan et al., 2013; Hampton and Nguyen, 2010).

The results obtained in this study are unique and to our knowledge not a single paper of flotation of precipitated particles by NBs has been published.

Thus, these NBs appear to interact with the amine precipitates (or flocs) as follows: i. Attachment (adhesion) at the precipitates (flocs)/solution interface; ii. Aggregation of the precipitates (flocs); iii. Entrainment or entrapment of the NBs followed by flotation of the aggregates. Figure 5.7 shows photomicrographs of amine precipitates in the presence and absence of NBs, showing their aggregation by the NBs and clearly depicting the floating aerated flocs. This phenomenon has also been found and published by our group on hydrophobic quartz fines (Calgaroto et al., 2015).

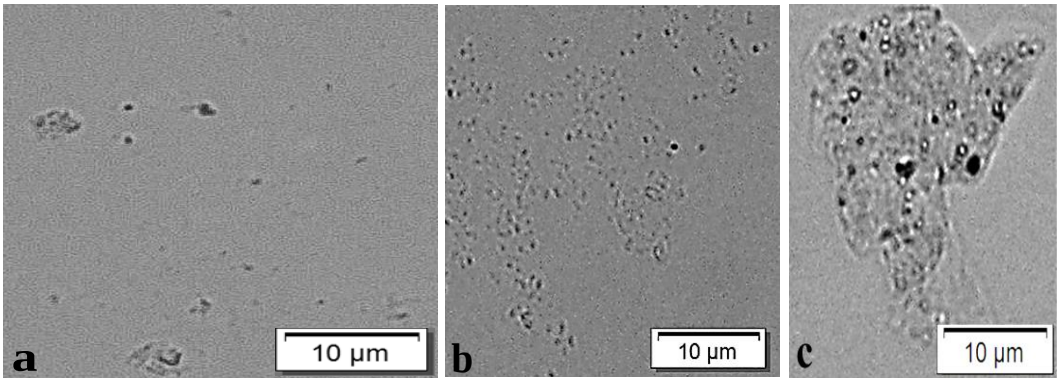

Figure 5.7. Photomicrographs of amine nano-precipitates of 500 mg.L^{-1} decyl-trimethyl-ether amine (Flotigam EDA 3B) at pH 10.8: a) nano-precipitates (40 – 500 nm) without NBs; b) nano-precipitates (40 – 500 nm) aggregated by NBs; c) amine floating precipitates with entrapped NBs.

5.3.3 Amine emission problems and legislation

According to Araujo et al. (2010), the degradation time of the dumped ether amines in iron ore tailings dams may be around 12 days depending on feed concentration, pH, light (ultraviolet irradiation) and acidity. Although this period may appear to be relatively short, the problems caused by those residual amines are not yet fully understood due to the continuous emission of nitrogen-bearing compounds in large quantities. In addition, there are two major risks involving the emission of amines:

1. The formation of toxic compounds such as nitrosamines (carcinogenic) through reactions between precursor amines and oxidants such as nitrites (Lin, 1990);
2. The amine-based carbon capture facilities that drain amines to the surface and underground waters constitute a new problem (SEPA, 2013).

However, there is still no specific legislation for the emission standards for amine compounds and studies report that a high rate of biodegradability (by bacteria) of alkylamines is associated with its concentration. Thus, values of amine concentration above 10 $mg.L^{-1}$ will inhibit bacterial growth that is responsible for amine degradation (Yoshimura et al., 1980). Comparing the amine concentration values usually found in Brazilian iron tailings dams (approximately 30 $mg.L^{-1}$), the ether amine residual concentration of 6 $mg.L^{-1}$ obtained in the bench scale studies may be considered a low concentration, which would permit the biodegradability by bacteria. On the basis of these findings, it appears that flotation with NBs has a good potential for treating mining effluent containing amines.

5.3.4 Final remarks

A number of recent studies have reported some advantages in mineral flotation in the presence of NBs and this work also shows benefits in the removal of a pollutant.

Authors from Kentucky State University (USA) claim that NBs increase the contact angles at the bubble-mineral particle interface and, subsequently, enhance the probability of bubble–particle attachment and stability (Fan and Tao, 2008; Fan et al., 2010 a, b, c, 2012, 2013; Sobhy, 2013; Sobhy and Tao 2013).

More, NBs would also enhance particle flotation recoveries at lower collector and frother dosages and at high kinetic flotation rate (Fan et al., 2012; Sobhy, 2013; Sobhy and Tao 2013).

Because of the novelty and efficiency on the removal of the toxic amines by flotation with NBs, this work will continue including the validation of the results at pilot scale in a column-like flotation cell, searching for the possibility of amine reuse and evaluation of general costs. A parallel contribution would be to assist environmental agencies in establishing emissions standard limits in ore mining operations.

Another challenge, important from an engineering viewpoint, is the sustainable generation of NBs at a high rate; this may be possible by optimizing the depressurization technique and exploring power acoustic or ultrasonic cavitation; blowing gas through turbulent flow (shearing) in cavitation tubes or fluidic oscillators, among others(Calgaroto et al., 2014; Kukizaki and Goto, 2006; Sobhy, 2013; Sobhy and Tao, 2013; Zimmerman et al., 2011).

5.4 CONCLUSIONS

Decyl–trimethyl-ether amine, employed on a large scale in the iron ore industry, precipitates at pH > 10.5 and their sizes range from nanometers to micrometers. The NBs aggregate the amine precipitates and float them efficiently. Flotation-separation with NBs depended on feed amine concentration, solution pH and flocculation of the precipitates. Conversely, the combination of MBs and NBs did not float the aggregates efficiently, due to the high rising velocities of the MBs which broke up some precipitates. The best results were 80% removal yielding a very low residual amine concentration in water, about 6 $mg.L^{-1}$. It is believed that flotation with NBs has a high potential in removing precipitates and light hydrophobic moieties.

5.5 ACKNOWLEDGMENTS

The authors would like to thank all the Brazilian Institutes supporting this research, namely CNPq, Fapergs and UFRGS. Special thanks are due to Monica Speck Cassola from Clariant for the amine samples and Prof. Adriana Pohlmann from the Chemistry Department at our University for her assistance with the optical microscope/camera. Special thanks to William LeBarre for her kind revision of the English; to all students (especially Luísa Heineck Neves and Marcio Nicknig) and to Dr. Katia Wilberg and Mr. Ramiro Etchepare, MSc, for their constant cooperative inputs and research help.

PARTE III

6. PRODUÇÃO CIENTÍFICO-TECNOLÓGICA ASSOCIADA À TESE

O estudo desenvolvido durante o doutorado, além dos três artigos científicos publicados em periódicos internacionais e apresentados nesse Plano de Tese de Doutorado, gerou uma quarta publicação dentro dos estudos de aplicações de NBs na flotação para remoção de poluentes:

- *Removal of sulfate ions by dissolved air flotation (DAF) following precipitation and flocculation.* **Amaral Filho, J., Azevedo, A., Etchepare, R. Rubio, J**. International Journal of Mineral Processing, v. 149, p. 1– 8, 2016.

Nesse artigo foi apresentado um estudo de remoção de sulfatos por precipitação-floculação-FAD, avaliando a flotação assistida por NBs como alternativa para o aumento da eficiência de flotação dos sólidos formados na precipitação de sulfato com policloreto de alumínio (PAC) e floculação com poliacrilamida catiônica. Os resultados demonstraram que a FAD é uma boa alternativa na remoção desses sólidos contendo sulfatos e que o processo parece estar limitado nos equilíbrios químicos das reações de precipitação do sulfato com espécies poliméricas de alumínio. O condicionamento com NBs apresentou leve melhora na remoção de sulfato, embora esse aumento de eficiência não tenha sido estatisticamente significante, devido ao fato de a FAD sem condicionamento de NBs já ter alcançado níveis elevados de remoção de precipitados de sulfato.

Artigos de Congressos

Ainda, diversos trabalhos foram apresentados em congressos e workshops internacionais, com os estudos realizados dentro do projeto de doutorado, com foco na caracterização e aplicação de NBs geradas por despressurização:

- *Featuring the nanobubbles scenarios in mining and mineral flotation*. **Azevedo, A., Etchepare, R., Paiva, M., Rosa, A. F., Rubio, J.** 24th World Mining Congress – Rio de Janeiro, Brasil. 18-21 October 2016. 24 th World Mining Congress Proceedings - Innovation in mining.

- *Nanobubbles: their role in dissolved air flotation.* **Etchepare, R., Azevedo, A., Rubio, J.** 7th International Conference on Flotation 2016 – Flotation for water and wastewater systems– Toulouse, França. 26-30 September 2016. Proceedings p. 338-346.
- *The role of nanobubbles in the flotation of minerals and mining wastewaters.* **Azevedo, A., Etchepare, R., Rosa, A. F., Rubio, J.** II Congreso Internacional de Flotación de Minerales – CD-ROM of the proceedings; dia 1. Lima, Peru. 22-24 Junho 2016.
- *Nanobolhas: geração, propriedades e aplicações ambientais.* **Azevedo, A., Calgaroto, S., Etchepare, R., Rubio, J.** In: 5º Congresso Internacional de Tecnologias para o Meio Ambiente. Evento integrante da Feira Internacional de Tecnologias para o Meio Ambiente - FIEMA, Bento Gonçalves-RS, Abril 2016.
- *Nanobubbles: generation, properties and environmental applications.* **Azevedo, A., Calgaroto, S., Etchepare, R., Rubio, J.** II International Congress of Environmental Science and Technology (SACyTA December 2015, Buenos Aires, Argentina); Proceedings p. 217-224.
- *La remoción de los iones de xantato por precipitación-flotación por aire disuelto (FAD).* **Etchepare R.; Azevedo, A., Oliveira, K., Rubio, J.** II International Congress of Environmental Science and Technology (SACyTA December 2015, Buenos Aires, Argentina).
- *Effect of the injection of nanobubbles on quartz flotation recoveries of fine particles.* **Calgaroto, S., Azevedo, A. and Rubio, J.** IMEC-International Minerals Engineering Congress 2014 (IMEC September 2014, San Luis Potosí, Mexico); Proceedings p 164-183.

Depósito de Patente

Como resultado da pesquisa na geração de nanobolhas de gases dispersas em líquido, foi gerado um produto tecnológico com depósito de patente no Instituto Nacional da propriedade Industrial (INPI, Número do Processo BR 10 2016 006081 8). A patente se refere a equipamento e processo de geração de nanobolhas dispersas em líquidos em alta concentração ($> 10^9$ NBs.mL^{-1}) para aplicações na engenharia ambiental e sanitária, microbiologia, agricultura e criação de animais aquáticos, processos da indústria química, de alimentos e bebidas que necessitam de aeração/gaseificação prolongada e eficiente.

7. CONSIDERAÇÕES FINAIS

O processo de flotação foi desenvolvido e vem sendo empregado há mais de 100 anos no beneficiamento de minérios, para recuperação de partículas minerais de interesse (Fuerstenau et al., 2007). Ao longo dessa história consagrada da flotação na área mineral, diversos desenvolvimentos tecnológicos e melhorias de processos foram implementados buscando aumento da recuperação de minérios de interesse e maior sustentabilidade do processo (eficiência energética, menor consumo de reagentes e de água de processo, entre outros).

Na área ambiental, no tratamento de águas e efluentes líquidos (remoção de poluentes e reuso de água) a flotação iniciou a ser empregada nos anos 60 e passou por diversos desenvolvimentos, principalmente relacionados aos métodos de geração de bolhas na FAD (com vasos saturadores ou bombas centrífugas multifásicas) e ao design das células de flotação (convencionais ou em coluna). Atualmente, são conhecidas aplicações da FAD em diversos tipos de efluentes líquidos e em águas para abastecimento urbano (Edzwald and Haarhoff, 2011; Edzwald, 2010; Rubio et al., 2002).

A diferença nestas aplicações está no tamanho e distribuição de tamanho de bolhas gerada: macrobolhas (0,6-2 mm) na flotação de minérios e microbolhas (40-100 μm) na flotação (separação) de poluentes (partículas, coloides, gotículas). Entretanto, a contribuição das NBs ainda é desconhecida da maioria dos engenheiros, pesquisadores e profissionais da área de flotação. Este fato se deve principalmente pela ausência e/ou desconhecimento de técnicas analíticas capazes de caracterizar e identificar as NBs, até então.

Nas últimas décadas, houve um avanço significativo da nanotecnologia e o desenvolvimento de técnicas de análise de partículas/bolhas mais avançadas, permitiu uma melhor compreensão das propriedades destas bolhas. Nos últimos anos, os estudos envolvendo a aplicação das NBs no processo de flotação avançaram de forma crescente, especialmente no setor mineral e poucos na área ambiental provavelmente pela falta de uma técnica de geração de soluções aquosas concentradas de NBs. Desse modo, a presente tese permitiu contribuir, com uma investigação aprofundada para aprimorar métodos de flotação com MBs e NBs, validada com aplicações em nível de bancada e contínuo. As fortalezas do estudo foram determinar as condições ótimas de processo de geração de uma alta concentração de NBs estáveis e com um elevado potencial para viabilizar diferentes aplicações.

Os resultados obtidos estimulam a utilização destas bolhas no desenvolvimento de técnicas e tecnologias na área de beneficiamentos de minérios e na área ambiental, na remoção de outros tipos de poluentes, entre eles:

i. No aumento da eficiência dos processos de beneficiamento de minérios, especialmente na recuperação das frações finas e ultrafinas;

ii. No tratamento de efluentes da mineração, na remoção de reagentes “coletores” de flotação de minérios (xantatos e derivados, aminas, ácidos graxos e íons diversos);

iii. Na petroquímica e na extração de petróleo no controle da emissão e reinjeção de águas produzidas;

iv. No setor de industrial e de mitigação da poluição aquosa urbana, no tratamento de águas de lavagem de carros, caminhões, ônibus, aviões, maquinaria industrial pesada.

Estudos futuros podem avaliar a injeção de bolhas na flotação usando bombas multifásicas geradoras de bolhas, de forma que sejam testadas e validadas em tempos longos e com diferentes tipos de águas de processo. As Figuras XX e XX apresentam exemplos destes fluxogramas propostos em aplicações futuras de flotação no tratamento de efluentes líquidos e no beneficiamento de minérios, respectivamente.

Figura 7.1. Fluxograma de processo de floculação-flotação para tratamento de efluentes líquidos com múltipla injeção de bolhas. [1]NBs geradas em vaso saturador com P_{sat} de 2 atm; [2]Geração conjunta de MBs e NBs em P_{sat} de 4 atm.

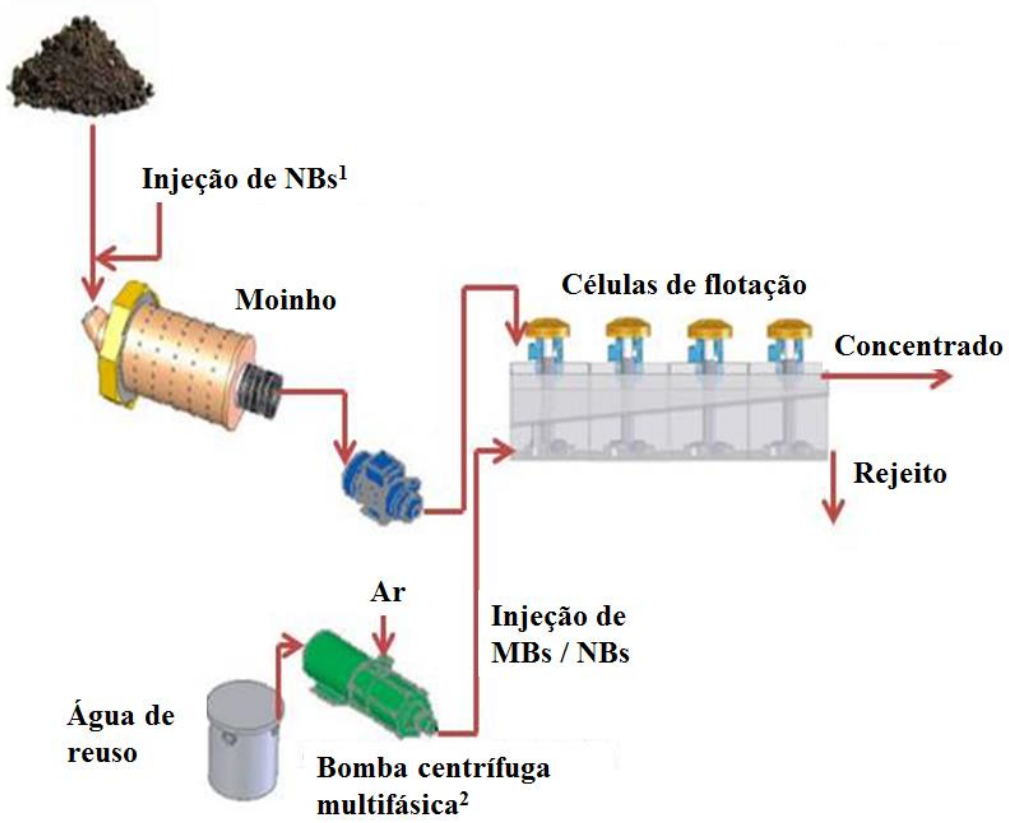

Figura 7.2. Fluxograma proposto de processo de beneficiamento de minérios por flotação com múltipla injeção de bolhas. [1]NBs geradas em vaso saturador com P_{sat} de 2 atm; [2]Geração conjunta de MBs e NBs em P_{sat} de 4 atm.

Assim, a pesquisa e inovação nos processos de flotação continuam nos setores acadêmicos e produtivos, buscando processos mais eficientes, tanto técnica como economicamente.

8. CONCLUSÕES

Os resultados obtidos no presente estudo permitem estabelecer as seguintes conclusões:

1. A concentração numérica de NBs geradas por despressurização em constritor de fluxo do tipo válvula agulha se mostrou inversamente proporcional à pressão de saturação e à tensão superficial do líquido, alcançando um valor máximo de 1,6 x 10^9 NBs.mL^{-1} em P_{sat} de 2,5 bar e T_{sup} = 49 mN.m^{-1} (solução de α-Terpineol 100 mg.L^{-1});
2. As NBs geradas por despressurização, em água deionizada e em solução de α-Terpineol (100 mg.L^{-1}) permaneceram estáveis, dispersas em meio líquido, sem mudanças significativas no seu tamanho médio e concentração numérica por um período de 14 dias;

3. O potencial zeta das NBs geradas em solução de α-Terpineol (100 mg.L^{-1}) apresentaram valores negativos na faixa de pH estudada, apresentando um valor de carga negativa baixa (-10 mV) em pH 3 e alcançando um valor de carga negativa elevado (-54 mV) em pH 8. O tamanho médio dessas NBs mostrou uma dependência com o potencial zeta, uma vez que bolhas menores (250 nm) foram encontradas em pH 8, em comparação com o tamanho das bolhas em pH 3 (530 nm).
4. O condicionamento de uma partícula de pirita em suspensão com alta concentração de NBs proporcionou uma maior eficiência de adesão de microbolhas na superfície da pirita, demonstrando o efeito de NBs na hidrofobização de partículas sólidas;
5. O condicionamento de NBs proporcionou um aumento de eficiência na recuperação de partículas finas de quartzo. Na amostra de quartzo com D32 de 8 μm, a recuperação de partículas aumentou de 75% para 87% quando foi utilizada uma etapa de condicionamento com NBs antes da flotação em tubo de Hallimond, na amostra com D32 de 34 μm, a recuperação de partículas aumentou de 67% para 84%;
6. O condicionamento de uma partícula de quartzo com NBs proporcionou o aumento do ângulo de contato bolha-partícula após a adesão de uma macrobolha. O ângulo de contato medido na ausência de NBs (com solução de amina 10^{-6} M) foi de 18°, enquanto que após o condicionamento com NBs, geradas em solução de amina de mesma concentração, o ângulo de contato medido foi de 46°;
7. Microfotografias realizadas em amostras de suspensão de partículas de quartzo demonstraram o efeito de agregação das partículas finas;
8. A presença de NBs no líquido reduziu a velocidade de ascensão de macrobolhas, aumentando o tempo de residência de bolhas no sistema de flotação. As velocidades de ascensão de macrobolhas medidas em água deionizada, solução de amina de 10^{-5} M e solução de amina de 5 x 10^{-5} M foram 4,8 cm.s^{-1}, 4,6 cm.s^{-1} e 2,6 cm.s^{-1}, respectivamente. Quando o líquido foi previamente enriquecido com NBs, esses valores de velocidade de ascensão medidos foram 3,9 cm.s^{-1}, 3,7 cm.s^{-1} e 1,4 cm.s^{-1}, respectivamente.
9. A precipitação de amina (decil-eter-amina) a pH 10,5 gera espécies sólidas com distribuição de tamanho ampla (200 nm – 250 μm) com 3 picos em 400 nm (precipitados nanométricos), em 2 μm (micro precipitados finos) e em 140 μm (micro precipitados);

10. Os precipitados de aminas apresentaram potencial zeta positivo em valores de pH abaixo de 10,8 (ponto isoelétrico), sugerindo uma maior instabilidade do sistema coloidal e agregação das partículas coloidais de aminas nesse pH;
11. A flotação desses precipitados de aminas com NBs isoladas foi mais eficiente em comparação com a FAD convencional em todos os casos estudados, de concentração inicial de amina variando entre 1,95 $mg.L^{-1}$ e 500 $mg.L^{-1}$, tanto com uso de uma etapa de floculação com policloreto de alumínio (PAC – 5 $mg.L^{-1}$) como sem floculação. A condição ótima de remoção de amina foi obtida com flotação com NBs isoladas e com uso de floculante, obtendo valores próximos de 80% de remoção em todas as faixas de concentração inicial de amina;
12. Microfotografias realizadas em amostras de suspensão de precipitados coloidais de aminas demonstraram o efeito de agregação das partículas na presença de NBs e a formação de "precipitados aerados" pelo aprisionamento de NBs no interior dos sólidos.

9. SUGESTÕES DE TRABALHOS FUTUROS

A pesquisa de geração de NBs deve continuar a fim de se obter métodos cada vez mais eficientes e sustentáveis de geração de dispersões aquosas de NBs, em alta taxa (concentração numérica e volumétrica de NBs) e baixo gasto energético, explorando os mecanismos de despressurização de corrente líquida saturada em gás, cavitação hidrodinâmica e cisalhamento de massa líquida contendo gases dissolvidos. Além de se obter condições de geração de NBs modificadas (carregadas positiva ou negativamente), para possibilitar um aumento do campo de pesquisa nas aplicações de NBs.

Nas aplicações de NBs nas áreas mineral e ambiental, o potencial tecnológico das NBs traz uma vasta possibilidade de estudos futuros, dos quais alguns estão citados abaixo:

Aplicações de NBs na área mineral:

- Estudos de flotação em bancada (células mecânicas) com diferentes sistemas minerais, utilizando injeção de MBs e NBs no processo;
- Estudos em escala piloto (contínuo e/ou semi-contínuo) com aplicação de flotação multibolhas no tratamento de minérios, com injeção de NBs nas etapas de moagem e condicionamento da polpa e injeção de MBs e NBs, em conjunto com macrobolhas, na coluna de flotação;

Aplicações de NBs na área ambiental:

- Geração, caracterização e aplicação de NBs de ozônio para oxidação de poluentes diversos em águas residuárias (industriais e urbanas) e para desinfecção de águas de abastecimento;
- Estudos de validação em escala piloto (contínuo ou semi-contínuo) de flotação com NBs (assistida com NBs e/ou NBs isoladas) para remoção de poluentes diversos (orgânicos e inorgânicos) em etapa de separação sólido-líquido no tratamento de efluentes;
- Uso de NBs de gases (ar ou ozônio) em processos mais limpos e sustentáveis de limpeza de superfícies sólidas;
- Uso de NBs de gases (ar ou ozônio) no *defouling* e/ou prevenção de *fouling* de membranas de tratamento de águas e efluentes ou da indústria química e alimentícia;
- Uso de NBs de ar ou oxigênio no tratamento biológico de efluentes, na aeração de sistemas aeróbios e no crescimento de micro-organismos específicos utilizados no tratamento de efluentes;

REFERÊNCIAS BIBLIOGRÁFICAS

Agarwal, A., 2005. An experimental study of nanobubbles on hydrophobic surfaces.

Agarwal, A., Ng, W.J., Liu, Y., 2011. Principle and applications of microbubble and nanobubble technology for water treatment. Chemosphere 84, 1175–80. doi:10.1016/j.chemosphere.2011.05.054

Ahmadi, R., Khodadadi, D.A., Abdollahy, M., Fan, M., 2014. Nano-microbubble flotation of fine and ultrafine chalcopyrite particles. Int. J. Min. Sci. Technol. 24, 559–566. doi:10.1016/j.ijmst.2014.05.021

An, H., Liu, G., Craig, V.S.J., 2015. Wetting of nanophases: Nanobubbles, nanodroplets and micropancakes on hydrophobic surfaces. Adv. Colloid Interface Sci. 222, 9–17. doi:10.1016/j.cis.2014.07.008

Araujo, D.M., Yoshida, M.I., Carvalho, C.F., 2009. Colorimetric determination of ether amine greases utilized in the flotation of iron ore. J. Anal. Chem. 64, 390–392. doi:10.1134/S1061934809040121

Araujo, D.M., Yoshida, M.I., Takahashi, J.A., Carvalho, C.F., Stapelfeldt, F., 2010. Biodegradation studies on fatty amines used for reverse flotation of iron ore. Int. Biodeterior. Biodegradation 64, 151–155. doi:10.1016/j.ibiod.2010.01.004

Attard, P., 2003. Nanobubbles and the hydrophobic attraction. Adv. Colloid Interface Sci. 104, 75–91. doi:10.1016/S0001-8686(03)00037-X

Attard, P., Moody, M.P., Tyrrell, J.W.G., 2002. Nanobubbles: the big picture. Phys. A Stat. Mech. its Appl. 314, 696–705. doi:10.1016/S0378-4371(02)01191-3

Baltar, C.A.M., De Araujo, J.M.M., Cunha, A.S.F., 2002. Estudo das condições para dessorção e reutilização de coletor na flotação de quartzo, in: XIX Encontro Nacional de Tratamento de Minérios E Metalurgia Extrativa. Recife-PE, pp. 241–246.

Berne, B.J., Pecora, R., 2000. Dynamic light scattering : with applications to chemistry, biology, and physics. Dover Publications.

Bunkin, N.F., Indukaev, K. V., Ignat'ev, P.S., 2007. Spontaneous self-organization of microbubbles in a liquid. J. Exp. Theor. Phys. 104, 486–498. doi:10.1134/S1063776107030156

Bunkin, N.F., Suyazov, N. V., Shkirin, A. V., Ignat'ev, P.S., Indukaev, K. V., 2009. Cluster structure of stable dissolved gas nanobubbles in highly purified water. J. Exp. Theor. Phys. 108, 800–816. doi:10.1134/S1063776109050082

Bunkin, N.F., Yurchenko, S.O., Suyazov, N. V, Shkirin, A. V, 2012. Structure of the nanobubble clusters of dissolved air in liquid media. J. Biol. Phys. 38, 121–52. doi:10.1007/s10867-011-9242-8

Calgaroto, S., 2014. Propriedades interfaciais de nanobolhas e estudos na flotação de quartzo e precipitados coloidais de amina. Dissertação de Mestrado, UFRGS, Porto Alegre.

Calgaroto, S., Azevedo, A., Rubio, J., 2016. Separation of amine-insoluble species by flotation with nano and microbubbles. Miner. Eng. 89, 24–29. doi:10.1016/j.mineng.2016.01.006

Calgaroto, S., Azevedo, A., Rubio, J., 2015. Flotation of quartz particles assisted by nanobubbles. Int. J. Miner. Process. 137, 64–70. doi:10.1016/j.minpro.2015.02.010

Calgaroto, S., Wilberg, K.Q., Rubio, J., 2014. On the nanobubbles interfacial properties and future applications in flotation. Miner. Eng. 60, 33–40. doi:10.1016/j.mineng.2014.02.002

Cavalli, R., Argenziano, M., Vigna, E., Giustetto, P., Torres, E., Aime, S., Terreno, E., 2015. Preparation and in vitro characterization of chitosan nanobubbles as theranostic agents. Colloids Surf. B. Biointerfaces 129, 39–46. doi:10.1016/j.colsurfb.2015.03.023

Cavalli, R., Bisazza, A., Lembo, D., 2013. Micro- and nanobubbles: a versatile non-viral platform for gene delivery. Int. J. Pharm. 456, 437–45. doi:10.1016/j.ijpharm.2013.08.041

Cavalli, R., Bisazza, A., Trotta, M., Argenziano, M., Civra, A., Donalisio, M., Lembo, D., 2012. New chitosan nanobubbles for ultrasound-mediated gene delivery: preparation and in vitro characterization. Int. J. Nanomedicine 7, 3309–18. doi:10.2147/IJN.S30912

Chan, C.U., Arora, M., Ohl, C.-D., 2015. Coalescence, Growth, and Stability of Surface-

Attached Nanobubbles. Langmuir 31, 7041–6. doi:10.1021/acs.langmuir.5b01599

Chan, C.U., Ohl, C.D., 2012. Total-internal-reflection-fluorescence microscopy for the study of nanobubble dynamics. Phys. Rev. Lett. 109, 1–5. doi:10.1103/PhysRevLett.109.174501

Chan, C.W., Siqueiros, E., Ling-Chin, J., Royapoor, M., Roskilly, A.P., 2015. Heat utilisation technologies: A critical review of heat pipes. Renew. Sustain. Energy Rev. 50, 615–627. doi:10.1016/j.rser.2015.05.028

Chaplin, M.F., 2007. The Memory of Water: an overview. Homeopathy 96, 143–50. doi:10.1016/j.homp.2007.05.006

Chaves, L.C., 2001. Estudo de resíduos sólidos gerados na flotação de minério de ferro: Quantificação e decomposição de aminas no meio ambiente. UFOP, Ouro Preto – MG.

Chen, H., Mao, H., Wu, L., Zhang, J., Dong, Y., Wu, Z., Hu, J., 2009. Defouling and cleaning using nanobubbles on stainless steel. Biofouling 25, 353–7. doi:10.1080/08927010902807645

Chen, K.-K., 2009. Bathing pool assembly with water full of nano-scale ozone bubbles for rehabilitation.

Craig, V.S.J., 2004. Bubble coalescence and specific-ion effects. Curr. Opin. Colloid Interface Sci. 9, 178–184. doi:10.1016/j.cocis.2004.06.002

Ebina, K., Shi, K., Hirao, M., Hashimoto, J., Kawato, Y., Kaneshiro, S., Morimoto, T., Koizumi, K., Yoshikawa, H., 2013. Oxygen and air nanobubble water solution promote the growth of plants, fishes, and mice. PLoS One 8, e65339. doi:10.1371/journal.pone.0065339

Edzwald, J., Haarhoff, J., 2011. Dissolved Air Flotation For Water Clarification, 1st ed. McGraw Hill Professional.

Edzwald, J.K., 2010. Dissolved air flotation and me. Water Res. 44, 2077–2106. doi:10.1016/j.watres.2009.12.040

Edzwald, J.K., 1995. Principles and applications of dissolved air flotation. Water Sci. Technol. 31, 1–23. doi:10.1016/0273-1223(95)00200-7

Englert, A.H., Rodrigues, R.T., Rubio, J., 2009. Dissolved air flotation (DAF) of fine quartz particles using an amine as collector. Int. J. Miner. Process. 90, 27–34. doi:10.1016/j.minpro.2008.10.001

Etchepare, R., Azevedo, A., Rubio, J., 2016. Nanobubbles: their role in dissolved air flotation, in: The 7th International Conference on Flotation for Water and Wastewater Systems, Flotation 2016. IWA Publishing, Toulouse, France, pp. 338–345.

Fan, M., Tao, D., 2008. A Study on Picobubble Enhanced Coarse Phosphate Froth Flotation. Sep. Sci. Technol.

Fan, M., Tao, D., Honaker, R., Luo, Z., 2010a. Nanobubble generation and its applications in froth flotation (part II): fundamental study and theoretical analysis. Min. Sci. Technol. 20, 159–177. doi:10.1016/S1674-5264(09)60179-4

Fan, M., Tao, D., Honaker, R., Luo, Z., 2010b. Nanobubble generation and its applications in froth flotation (part IV): Mechanical cells and specially designed column flotation of coal. Min. Sci. Technol. 20, 641–671. doi:10.1016/S1674-5264(09)60259-3

Fan, M., Tao, D., Honaker, R., Luo, Z., 2010c. Nanobubble generation and its applications in froth flotation (part III): specially designed laboratory scale column flotation of phosphate. Min. Sci. Technol. 20, 317–338. doi:10.1016/S1674-5264(09)60205-2

Fan, M., Tao, D., Honaker, R., Luo, Z., 2010d. Nanobubble generation and its application in froth flotation (part I): nanobubble generation and its effects on properties of microbubble and millimeter scale bubble solutions. Min. Sci. Technol. 20, 1–19. doi:10.1016/S1674-5264(09)60154-X

Fan, M., Tao, D., Zhao, Y., Honaker, R., 2013. Effect of nanobubbles on the flotation of different sizes of coal particle. Miner. Metall. Process. J. 30, 157–161.

Fan, M., Zhao, Y., Tao, D., 2012. Fundamental studies of nanobubble generation and applications in flotation, in: Separation Technologies for Minerals, Coal and Earth Resources. Society for Mining, Metallurgy and Exploration - SME, Littleton, pp. 457–469.

Feng, D., Aldrich, C., 1999. Effect of particle size on flotation performance of complex sulphide ores. Miner. Eng. 12, 721–731. doi:10.1016/S0892-6875(99)00059-X

Féris, L.A., Rubio, J., 1999. Dissolved air flotation (DAF) performance at low saturation pressures. Filtr. Sep. 36, 61–65. doi:10.1016/S0015-1882(99)80223-7

Filipe, V., Hawe, A., Jiskoot, W., 2010. Critical evaluation of Nanoparticle Tracking Analysis (NTA) by NanoSight for the measurement of nanoparticles and protein aggregates. Pharm. Res. 27, 796–810. doi:10.1007/s11095-010-0073-2

Fraim, M., Jakhete, S., 2015. Electrolytic cell with advanced oxidation process and electro catalytic paddle electrode. 8945353.

Franzidis, J.P., Manlapig, E.V., 1999. A new, comprehensive, and usefulmodel for flotation, in: Parekh, B.K., Miller, J.D. (Eds.), Advances in Flotation Technology. SME, Denver, pp. 413–423.

Fuerstenau, M.C., Jameson, G.J., Yoon, R.-H., 2007. Froth Flotation: A Century of Innovation.

Fuerstenau, M.C., Miller, J.D., Kuhn, M.C., 1985. Chemistry of flotation. Published by Society of Mining Engineers of the American Institute of Mining, Metallurgical and Petroleum Engineers.

Ghadimkhani, A., Zhang, W., Marhaba, T., 2016. Ceramic membrane defouling (cleaning) by air Nano Bubbles. Chemosphere 146, 379–84. doi:10.1016/j.chemosphere.2015.12.023

Gontijo, C., Fornasiero, D., Ralston, J., 2008. The Limits of Fine and Coarse Particle Flotation. Can. J. Chem. Eng. 85, 739–747. doi:10.1002/cjce.5450850519

Gray-Weale, A., Beattie, J.K., 2009. An explanation for the charge on water's surface. Phys. Chem. Chem. Phys. 11, 10994–1005. doi:10.1039/b901806a

Gurung, A., Dahl, O., Jansson, K., 2016. The fundamental phenomena of nanobubbles and their behavior in wastewater treatment technologies. Geosystem Eng. 19, 133–142. doi:10.1080/12269328.2016.1153987

Hampton, M.A., Nguyen, A. V., 2009. Accumulation of dissolved gases at hydrophobic surfaces in water and sodium chloride solutions: Implications for coal flotation. Miner. Eng. 22, 786–792. doi:10.1016/j.mineng.2009.02.006

Hampton, M.A., Nguyen, A. V, 2010. Nanobubbles and the nanobubble bridging capillary force. Adv. Colloid Interface Sci. 154, 30–55. doi:10.1016/j.cis.2010.01.006

Hayakumo, S., Arakawa, S., Mano, Y., Izumi, Y., 2013. Clinical and microbiological effects of ozone nano-bubble water irrigation as an adjunct to mechanical subgingival debridement in periodontitis patients in a randomized controlled trial. Clin. Oral Investig. 17, 379–388. doi:10.1007/s00784-012-0711-7

Hayakumo, S., Arakawa, S., Takahashi, M., Kondo, K., Mano, Y., Izumi, Y., 2014. Effects of ozone nano-bubble water on periodontopathic bacteria and oral cells - in vitro studies. Sci. Technol. Adv. Mater. 15, 55003. doi:10.1088/1468-6996/15/5/055003

Heiskanen, K., 2000. On the relationship between flotation rate and bubble surface area flux. Miner. Eng. 13, 141–149. doi:10.1016/S0892-6875(99)00160-0

Honaker, R.Q., Mohanty, M.K., 1996. Enhanced column flotation performance for fine coal cleaning. Miner. Eng. 9, 931–945. doi:10.1016/0892-6875(96)00085-4

Honaker, R.Q., Wang, D., Ho, K., 1996. Application of the Falcon Concentrator for fine coal cleaning. Miner. Eng. 9, 1143–1156. doi:10.1016/0892-6875(96)00108-2

Hou, L., Yorulmaz, M., Verhart, N.R., Orrit, M., 2015. Explosive formation and dynamics of vapor nanobubbles around a continuously heated gold nanosphere. New J. Phys. 17,

13050. doi:10.1088/1367-2630/17/1/013050

Hunter, R.J., 1981. Zeta Potential in Colloid Science, Zeta Potential in Colloid Science. Elsevier. doi:10.1016/B978-0-12-361961-7.50007-9

Jameson, G.J., Manlapig, E.V., 1991. Applications of the Jameson flotation cell, in: Intemacional Conference on Column Rotation. Ontario, Canada, pp. 675–687.

Jameson, G.J., Nguyen, A., Ata, S., 2007. The flotation of fine and coarse particles, in: Froth Flotation: A Century of Innovation. SME, pp. 339–372.

Jia, W., Ren, S., Hu, B., 2013. Effect of Water Chemistry on Zeta Potential of Air Bubbles. Int. J. Electrochem. Sci 8, 5828–5837.

Karhu, M., Leiviskä, T., Tanskanen, J., 2014. Enhanced DAF in breaking up oil-in-water emulsions. Sep. Purif. Technol. 122, 231–241. doi:10.1016/j.seppur.2013.11.007

Karpitschka, S., Dietrich, E., Seddon, J.R.T., Zandvliet, H.J.W., Lohse, D., Riegler, H., 2012. Nonintrusive optical visualization of surface nanobubbles. Phys. Rev. Lett. 109, 1–5. doi:10.1103/PhysRevLett.109.066102

Kazuyuki, Y., Kazuyuki, S., Kazumi, C., 2010. Waste water treatment method and waste water treatment apparatus. US7641798 B2.

Kerfoot, W., 2015. Enhanced Reactive Zone. US 2015 0151993 A1.

Kerfoot, W., 2014. Nano-bubble generator and treatments. US 2014/0339143.

Kheir, J.N., Scharp, L.A., Borden, M.A., Swanson, E.J., Loxley, A., Reese, J.H., Black, K.J., Velazquez, L.A., Thomson, L.M., Walsh, B.K., Mullen, K.E., Graham, D.A., Lawlor, M.W., Brugnara, C., Bell, D.C., McGowan, F.X., 2012. Oxygen Gas-Filled Microparticles Provide Intravenous Oxygen Delivery. Sci. Transl. Med. 4, 140ra88-140ra88. doi:10.1126/scitranslmed.3003679

King, R.P., 1982. Flotation of fine particles. 217–219 (Johannesburg)., in: King, R.P. (Ed.), Principles of Flotation. South Africa Institute of Mining and Metallurgy, Johannesbourg, pp. 217–219.

Kukizaki, M., Goto, M., 2006. Size control of nanobubbles generated from Shirasu-porous-glass (SPG) membranes. J. Memb. Sci. 281, 386–396. doi:10.1016/j.memsci.2006.04.007

Laskowski, J.S., 2013. From amine molecules adsorption to amine precipitate transport by bubbles: A potash ore flotation mechanism. Miner. Eng. 45, 170–179. doi:10.1016/j.mineng.2013.02.010

Laskowski, J.S., 1989. The colloid chemistry and flotation properties of primary aliphatic amines, in: Sastry, K., Fuerstenau, M.C. (Eds.), Challenges in Mineral Processing. AIME,

pp. 15–34.

Li, H., Hu, L., Song, D., Al-Tabbaa, A., 2013. Subsurface transport behavior of micro-nano bubbles and potential applications for groundwater remediation. Int. J. Environ. Res. Public Health 11, 473–86. doi:10.3390/ijerph110100473

Li, H., Hu, L., Song, D., Lin, F., 2014. Characteristics of micro-nano bubbles and potential application in groundwater bioremediation. Water Environ. Res. 86, 844–51.

Lima, E.R.A., Boström, M., Sernelius, B.E., Horinek, D., Netz, R.R., Biscaia, E.C., Kunz, W., Tavares, F.W., 2008. Forces between air-bubbles in electrolyte solution. Chem. Phys. Lett. 458, 299–302. doi:10.1016/j.cplett.2008.04.099

Lin, J.K., 1990. Nitrosamines as potential environmental carcinogens in man. Clin. Biochem. 23, 67–71.

Liu, G., Craig, V.S.J., 2009. Improved cleaning of hydrophilic protein-coated surfaces using the combination of Nanobubbles and SDS. ACS Appl. Mater. Interfaces 1, 481–7. doi:10.1021/am800150p

Liu, G., Wu, Z., Craig, V.S.J., 2008. Cleaning of protein-coated surfaces using nanobubbles: An investigation using a Quartz Crystal Microbalance. J. Phys. Chem. C 112, 16748–16753. doi:10.1021/jp805143c

Liu, S., Enari, M., Kawagoe Yoshinori, Makino, Y., Oshita, S., 2012. Properties of the water containing nanobubbles as a new technology of the acceleration of physiological activity. Elsevier Chem. Eng. Sci. 93, 250–256.

Liu, S., Kawagoe, Y., Makino, Y., Oshita, S., 2013. Effects of nanobubbles on the physicochemical properties of water: The basis for peculiar properties of water containing nanobubbles. Chem. Eng. Sci. 93, 250–256. doi:10.1016/j.ces.2013.02.004

Liu, Y., Tourbin, M., Lachaize, S., Guiraud, P., 2012. Flotation separation of SiO2 nanoparticles from waters, in: The 6th International IWA Conference on Flotation for Water and Wastewater Systems. New York.

Lou, S.-T., Ouyang, Z.-Q., Zhang, Y., Li, X.-J., Hu, J., Li, M.-Q., Yang, F.-J., 2000. Nanobubbles on solid surface imaged by atomic force microscopy. J. Vac. Sci. Technol. B Microelectron. Nanom. Struct. 18, 2573. doi:10.1116/1.1289925

Lukianova-Hleb, E.Y., Campbell, K.M., Constantinou, P.E., Braam, J., Olson, J.S., Ware, R.E., Sullivan, D.J., Lapotko, D.O., 2014a. Hemozoin-generated vapor nanobubbles for transdermal reagent- and needle-free detection of malaria. Proc. Natl. Acad. Sci. U. S. A. 111, 900–5. doi:10.1073/pnas.1316253111

Lukianova-Hleb, E.Y., Mutonga, M.B.G., Lapotko, D.O., 2012. Cell-specific multifunctional processing of heterogeneous cell systems in a single laser pulse treatment. ACS Nano 6, 10973–81. doi:10.1021/nn3045243

Lukianova-Hleb, E.Y., Ren, X., Sawant, R.R., Wu, X., Torchilin, V.P., Lapotko, D.O., 2014b. On-demand intracellular amplification of chemoradiation with cancer-specific plasmonic nanobubbles. Nat. Med. 20, 778–84. doi:10.1038/nm.3484

Mai, L., Yao, A., Li, J., Wei, Q., Yuchi, M., He, X., Ding, M., Zhou, Q., 2013. Cyanine 5.5 Conjugated Nanobubbles as a Tumor Selective Contrast Agent for Dual Ultrasound-Fluorescence Imaging in a Mouse Model. PLoS One 8, 1–10. doi:10.1371/journal.pone.0061224

Malvern, 2014. Webinar: Nanobubbles, separating fact from fiction. London, UK.

Miller, J.., Hu, Y., Veeramasuneni, S., Lu, Y., 1999. In-situ detection of butane gas at a hydrophobic silicon surface. Colloids Surfaces A Physicochem. Eng. Asp. 154, 137–147. doi:10.1016/S0927-7757(98)00891-7

Miller, J.D., Hu, Y., Veeramasuneni, S., Lu, Y., 1999. In-situ detection of butane gas at a hydrophobic silicon surface. Colloids Surfaces A Physicochem. Eng. Asp. 154, 137–147. doi:10.1016/S0927-7757(98)00891-7

Najafi, A.S., Drelich, J., Yeung, A., Xu, Z., Masliyah, J., 2007. A novel method of measuring electrophoretic mobility of gas bubbles. J. Colloid Interface Sci. 308, 344–350. doi:10.1016/j.jcis.2007.01.014

Nakashima, T., Kobayashi, Y., Hirata, Y., 2012. Method to exterminate blue-green algae in a large pond and to improve plant growth by micro-nano bubbles in activated water. Acta Hortic.

Neder, E.E., Leal Filho, L.S., 2005. O uso de aminas graxas e seus derivados na flotação de minérios brasileiros, in: XXI Encontro Nacional de Tratamento de Minérios E Metalurgia Extrativa – ENTMME. Natal-RN, pp. 395–404.

Newsome, L.D., Johnson, D.E., Lipnick, R.L., Broderius, S.J., Russom, C.L., 1991. A QSAR study of the toxicity of amines to the fathead minnow. Sci. Total Environ. 109–110, 537–551. doi:10.1016/0048-9697(91)90207-U

Oh, S.H., Han, J.G., Kim, J.-M., 2015. Long-term stability of hydrogen nanobubble fuel. Fuel 158, 399–404. doi:10.1016/j.fuel.2015.05.072

Ohgaki, K., Khanh, N.Q., Joden, Y., Tsuji, A., Nakagawa, T., 2010. Physicochemical approach to nanobubble solutions. Chem. Eng. Sci. 65, 1296–1300. doi:10.1016/j.ces.2009.10.003

Oliveira, C.R., Rubio, J., 2009. Isopropylxanthate ions uptake by modified natural zeolite and removal by dissolved air flotation. Int. J. Miner. Process. 90, 21–26. doi:10.1016/j.minpro.2008.09.006

Oshita, S., Liu, S., 2013. Nanobubble Characteristics and Its Application to Agriculture and Foods, in: Proceedings of AFHW 2013 International Symposium on Agri-Foods for Health and Wealth. Bangkok, Thailand, pp. 23–32.

Parker, J.L., Claesson, P.M., Attard, P., 1994. Bubbles, cavities, and the long-ranged attraction between hydrophobic surfaces. J. Phys. Chem. 98, 8468–8480. doi:10.1021/j100085a029

Peng, H., Birkett, G.R., Nguyen, A. V, 2015. Progress on the Surface Nanobubble Story: What is in the bubble? Why does it exist? Adv. Colloid Interface Sci. 222, 573–80. doi:10.1016/j.cis.2014.09.004

Perera, R.H., Solorio, L., Wu, H., Gangolli, M., Silverman, E., Hernandez, C., Peiris, P.M., Broome, A.-M., Exner, A.A., 2014. Nanobubble ultrasound contrast agents for enhanced delivery of thermal sensitizer to tumors undergoing radiofrequency ablation. Pharm. Res. 31, 1407–17. doi:10.1007/s11095-013-1100-x

Perera, R.H., Solorio, L., Wu, H., Gangolli, M., Silverman, E., Hernandez, C., Peiris, P.M., Broome, A.M., Exner, A. a., 2014. Nanobubble ultrasound contrast agents for enhanced delivery of thermal sensitizer to tumors undergoing radiofrequency ablation. Pharm. Res. 31, 1407–1417. doi:10.1007/s11095-013-1100-x

Peres, A., Agarwal, N., Bartalini, N., Beda, D., 2000. Environmental impact of an etheramine utilized as flotation collector., in: 7th International Mine Water Association Congress. IMWA, Ustron, Poland, pp. 464–471.

Phan, C.M., Nguyen, A. V, Miller, J.D., Evans, G.M., Jameson, G.J., 2003. Investigations of bubble–particle interactions. Int. J. Miner. Process. 72, 239–254. doi:10.1016/S0301-7516(03)00102-9

Polman, A., 2013. Solar steam nanobubbles. ACS Nano 7, 15–8. doi:10.1021/nn305869y

Rangharajan, K.K., Kwak, K.J., Conlisk, a. T., Wu, Y., Prakash, S., 2015. Effect of surface modification on interfacial nanobubble morphology and contact line tension. Soft Matter. doi:10.1039/C5SM00583C

Rodrigues, R.T., Rubio, J., 2007. DAF-dissolved air flotation: Potential applications in the mining and mineral processing industry. Int. J. Miner. Process. 82, 1–13. doi:10.1016/j.minpro.2006.07.019

Rodrigues, R.T., Rubio, J., 2003. New basis for measuring the size distribution of bubbles.

Miner. Eng. 16, 757–765. doi:10.1016/S0892-6875(03)00181-X

Rubio, J., Capponi, F., Matiolo, E., Nunes, D., Guerrero, C.P., Berkowitz, G., 2003. Advances in flotation of mineral fines., in: Proceedings XXII International Mineral Processing Congress (IMPC). Cape Town - South Africa, pp. 1014–1022.

Rubio, J., Souza, M.., Smith, R.., 2002. Overview of flotation as a wastewater treatment technique. Miner. Eng. 15, 139–155. doi:10.1016/S0892-6875(01)00216-3

Schenk, H.J., Steppe, K., Jansen, S., 2015. Nanobubbles: a new paradigm for air-seeding in xylem. Trends Plant Sci. 20, 199–205. doi:10.1016/j.tplants.2015.01.008

Schubert, H., 2005. Nanobubbles, hydrophobic effect, heterocoagulation and hydrodynamics in flotation. Int. J. Miner. Process. 78, 11–21. doi:10.1016/j.minpro.2005.07.002

Schultz, T.W., Wilke, T.S., Bryant, S.E., Hosein, L.M., 1991. QSARs for selected aliphatic and aromatic amines. Sci. Total Environ. 109–110, 581–7.

Seddon, J.R.T., Zandvliet, H.J.W., Lohse, D., 2011. Knudsen gas provides nanobubble stability. Phys. Rev. Lett. 107, 2–5. doi:10.1103/PhysRevLett.107.116101

SEPA, 2013. Scottish Environment Protection Agency. Review of Amine Emissions from Carbon Capture Systems. Scotland.

Sivamohan, R., 1990. The problem of recovering very fine particles in mineral processing — A review. Int. J. Miner. Process. 28, 247–288. doi:10.1016/0301-7516(90)90046-2

Smith, R.W., Akhtar, S., 1976. Cationic flotation of oxide and silicates, flotation., in: Fuerstenau, M.C. (Ed.), A. M. Gaudin Memorial Volume, Vol. 1. AIME, New York.

Sobhy, A., Tao, D., 2013. High-Efficiency Nanobubble Coal Flotation. Int. J. Coal Prep. Util. 33, 242–256. doi:10.1080/19392699.2013.810623

Sobhy, a, Honaker, R., Tao, D., 2013. Nanobubble Column Flotation for More Efficient Coal Recovery 507, 1–7.

Sobhy, S.A., 2013. Cavitation nanobubble enhanced flotation process for more efficient coal recovery. Thesis Diss. Eng. Kentucky State University.

Sobhy, Tao, D., 2013. Nanobubble column flotation of fine coal particles and associated fundamentals. Int. J. Miner. Process. 124, 109–116. doi:10.1016/j.minpro.2013.04.016

Solari, J.A., Rubio, J., 1984. Effect of polymeric flocculants on solid liquid separation by dissolved air flotation., in: Jone, M.J.J., Oblatt, R. (Eds.), Reagents in Minerals Industry. IMM, London, UK, pp. 87–91.

Subrahmanyam, T.V., Forssberg, K.S.E., 1990. Fine particles processing: shear-flocculation and carrier flotation — a review. Int. J. Miner. Process. 30, 265–286. doi:10.1016/0301-

7516(90)90019-U

Szatkowski, M., Freyberger, W.L., 1985. Kinetics of flotation with fine bubbles. Trans Inst Min Met. Sect C 94, 61–70.

Takahashi, M., 2005. Zeta potential of microbubbles in aqueous solutions: electrical properties of the gas-water interface. J. Phys. Chem. B 109, 21858–21864. doi:10.1021/jp0445270

Takahashi, M., Chiba, K.M., 2007. Oxygen Nanobubble Water and Method of Producing the Same. US20070286795.

Takahashi, T., Miyahara, T., Mochizuki, H., 1979. Fundamental study of bubble formation in dissolved air pressure flotation. J. Chem. Eng. Japan 12, 275–280. doi:10.1252/jcej.12.275

Tao, D., 2005. Role of Bubble Size in Flotation of Coarse and Fine Particles—A Review. Sep. Sci. Technol. 39, 741–760. doi:10.1081/SS-120028444

Tasaki, T., Wada, T., Baba, Y., Kukizaki, M., 2009a. Degradation of Surfactants by an Integrated Nanobubbles/VUV Irradiation Technique. Ind. Eng. Chem. Res. 48, 4237–4244. doi:10.1021/ie801279b

Tasaki, T., Wada, T., Baba, Y., Kukizaki, M., 2009b. Degradation of surfactants by an integrated nanobubbles/vuv irradiation technique. Ind. Eng. Chem. Res. 48, 4237–4244. doi:10.1021/ie801279b

Tsai, J.C., Kumar, M., Chen, S.Y., Lin, J.G., 2007. Nano-bubble flotation technology with coagulation process for the cost-effective treatment of chemical mechanical polishing wastewater. Sep. Purif. Technol. 58, 61–67. doi:10.1016/j.seppur.2007.07.022

Ushida, A., Hasegawa, T., Nakajima, T., Uchiyama, H., Narumi, T., 2012a. Drag reduction effect of nanobubble mixture flows through micro-orifices and capillaries. Exp. Therm. Fluid Sci. 39, 54–59. doi:10.1016/j.expthermflusci.2012.01.008

Ushida, A., Hasegawa, T., Takahashi, N., Nakajima, T., Murao, S., Narumi, T., Uchiyama, H., 2012b. Effect of mixed nanobubble and microbubble liquids on the washing rate of cloth in an alternating flow. J. Surfactants Deterg. 15, 695–702. doi:10.1007/s11743-012-1348-x

Ushikubo, F.Y., Furukawa, T., Nakagawa, R., Enari, M., Makino, Y., Kawagoe, Y., Shiina, T., Oshita, S., 2010. Evidence of the existence and the stability of nano-bubbles in water. Colloids Surfaces A Physicochem. Eng. Asp. 361, 31–37. doi:10.1016/j.colsurfa.2010.03.005

Weijs, J.H., Lohse, D., 2013. Why Surface Nanobubbles Live for Hours. Phys. Rev. Lett. 110, 54501. doi:10.1103/PhysRevLett.110.054501

Wu, Z., Chen, H., Dong, Y., Mao, H., Sun, J., Chen, S., Craig, V.S.J., Hu, J., 2008. Cleaning using nanobubbles: defouling by electrochemical generation of bubbles. J. Colloid Interface Sci. 328, 10–4. doi:10.1016/j.jcis.2008.08.064

Xing, Z., Wang, J., Ke, H., Zhao, B., Yue, X., Dai, Z., Liu, J., 2010. The fabrication of novel nanobubble ultrasound contrast agent for potential tumor imaging. Nanotechnology 21, 145607. doi:10.1088/0957-4484/21/14/145607

Yang, S., Duisterwinkel, A., 2011a. Removal of nanoparticles from plain and patterned surfaces using nanobubbles. Langmuir 27, 11430–5. doi:10.1021/la2010776

Yang, S., Duisterwinkel, A., 2011b. Removal of nanoparticles from plain and patterned surfaces using nanobubbles. Langmuir 27, 11430–5. doi:10.1021/la2010776

Yoon, R.-H., 2000. The role of hydrodynamic and surface forces in bubble–particle interaction. Int. J. Miner. Process. 58, 129–143. doi:10.1016/S0301-7516(99)00071-X

Yoon, R.-H., 1999. Bubble–particle interactions in flotation, in: Parekh, B.K., Miller, J.D. (Eds.), Advances in Flotation Technology. SME, Denver, pp. 95–112.

Yoon, R.-H., 1993. Microbubble flotation. Miner. Eng. 6, 619–630. doi:10.1016/0892-6875(93)90116-5

Yoon, R.H., Luttrell, G.H., 1994. Microcel TM column flotation scale-up and plant practice., in: 26th Annual Meeting Canadian Mineral Processing. CIM, p. paper 12.

Yoshimura, K., Machida, S., Masuda, F., 1980. Biodegradation of long chain alkylamines. J. Am. Oil Chem. Soc. 57, 238–241. doi:10.1007/BF02673948

Zhang, X., Chan, D.Y.C., Wang, D., Maeda, N., 2013. Stability of interfacial nanobubbles. Langmuir 29, 1017–23. doi:10.1021/la303837c

Zhang, X.H., Maeda, N., Craig, V.S.J., 2006. Physical properties of nanobubbles on hydrophobic surfaces in water and aqueous solutions. Langmuir 22, 5025–35. doi:10.1021/la0601814

Zheng, R., Yin, T., Wang, P., Zheng, R., Zheng, B., Cheng, D., Zhang, X., Shuai, X.-T., 2012. Nanobubbles for enhanced ultrasound imaging of tumors. Int. J. Nanomedicine 895. doi:10.2147/IJN.S28830

Zhou, Z.A., Xu, Z., Finch, J.A., 1994. On the role of cavitation in particle collection during flotation - a critical review. Miner. Eng. 7, 1073–1084. doi:10.1016/0892-6875(94)00053-0

Zhou, Z.A., Xu, Z., Finch, J.A., Hu, H., Rao, S.R., 1997. Role of hydrodynamic cavitation in fine particle flotation. Int. J. Miner. Process. 51, 139–149. doi:10.1016/S0301-

7516(97)00026-4

Zhu, J., An, H., Alheshibri, M., Liu, L., Terpstra, P.M.J., Liu, G., Craig, V.S.J., 2016. Cleaning with Bulk Nanobubbles. Langmuir 32, 11203–11211. doi:10.1021/acs.langmuir.6b01004

Zimmerman, W.B., Tesař, V., Bandulasena, H.C.H., 2011. Towards energy efficient nanobubble generation with fluidic oscillation. Curr. Opin. Colloid Interface Sci. 16, 350–356. doi:10.1016/j.cocis.2011.01.010